ESC European Society of Cardiology

European Heart Journal - Imaging Methods and Practice (2026) **4**, qyaf157
https://doi.org/10.1093/ehjimp/qyaf157

SPECIAL ARTICLE
Nuclear cardiology

Patient-centric performance and interpretation of positron emission tomography /computed tomography myocardial perfusion imaging: a clinical consensus statement of the European Association of Cardiovascular Imaging of the European Society of Cardiology

Bryan Abadie [1,*], Riccardo Liga [2], Ronny R. Buechel [3], Andreas A. Giannopoulos[3], María Nazarena Pizzi [4], Albert Roque [4], Ricardo Geronazzo[4], Fabien Hyafil[5,6], Juhani Knuuti[7], Antti Saraste [7], Riemer H.J.A. Slart[8,9], Paul Cremer[10], Richard Weinberg[10], Maria João Vidigal Ferreira[11], Alessia Gimelli[12], and Wael A. Jaber[1]

[1]Section of Cardiovascular Imaging, Department of Cardiovascular Medicine, Heart, Vascular, and Thoracic Institute, Cleveland Clinic Foundation, 9500 Euclid Avenue, J1-5 Main Campus, Cleveland, OH 44195, USA
[2]University of Pisa, Pisa, Italy
[3]Department of Nuclear Medicine, Cardiac Imaging, University and University Hospital of Zurich, Zurich, Switzerland
[4]University Hospital Vall d'Hebron, Barcelona, Spain
[5]Department of Nuclear Medicine, European Hospital Georges Pompidou, Paris, France
[6]Paris Research Cardiovascular Center, University of Paris, Paris, France
[7]Turku University Hospital and University of Turku, Turku, Finland
[8]Department of Nuclear Medicine and Molecular Imaging, University of Groningen, University Medical Center Groningen, Groningen, The Netherlands
[9]Biomedical Photonic Imaging Group, University of Twente, Enschede, The Netherlands
[10]Department of Medicine, Northwestern University, Chicago, IL, USA
[11]Institute for Nuclear Sciences Applied to Health, University of Coimbra, Coimbra, Portugal
[12]Imaging Department, Toscana Gabriele Monasterio Foundation, Pisa, Italy

Received 25 November 2025; accepted after revision 5 December 2025; online publish-ahead-of-print 13 January 2026

Abstract

Positron emission tomography (PET) is the most advanced myocardial perfusion (MPI) technique for the non-invasive assessment of coronary artery disease and its many manifestations, including ischaemia, hibernation, and scar. This comprehensive overview aims to empower clinicians, technicians, and patients with clear, structured knowledge on performing and

* Corresponding author. E-mail: abadieb@ccf.org

interpreting PET MPI. This document will describe stress protocols, patient preparation, tracer pharmacodynamics and nuclear properties, camera capabilities, post-acquisition processing, and a comprehensive and clear reporting system for both perfusion and viability imaging.

Keywords positron emission tomography myocardial perfusion • cardiac stress testing • viability imaging

Introduction

Positron emission tomography (PET) myocardial perfusion imaging (MPI) using radioactive tracers has become a well-established, non-invasive modality for the assessment of coronary artery disease (CAD). Over the course of the last several decades, new tracers, cameras, computerized algorithms, and stress protocols have been introduced and endorsed by various cardiac and imaging societies. Therefore, a novel clinical consensus statement is needed to introduce these topics and highlight European and American procedural differences with a patient-centric educational focus.

We will present a concise and clinically relevant document with visual aids that will cover the performance of PET MPI for patients with suspected or known coronary artery disease. This document sought to integrate knowledge from experts in both Europe and the USA, while incorporating the European Society of Cardiology (ESC) and American College of Cardiology guidelines, as well as best practice guidance from the American Society of Nuclear Cardiology and the European Association of Cardiovascular Imaging of the ESC.[1–3]

This document and its figures are meant to be a daily reference for patients and imaging centres to perform these tests, as well as a digestible introduction to new practitioners of PET MPI. In particular, this document aims to be complementary to dense procedural manuals, which are only accessible to experts, as well as larger guidelines on chronic coronary syndromes, which are test agnostic. This document will describe stress protocols, patient preparation, tracer pharmacodynamics and nuclear properties, camera capabilities, post-acquisition processing, and a comprehensive and clear reporting system for both perfusion and viability imaging. We also aimed to enhance a patient-centric approach by using various visual cartoons that can be shown and explained to patients. We have structured this paper to be helpful to a wide range of people, with the recognition that the relevance or comprehension of certain sections may vary depending on level of training. A simplified set of key points has been included in the Supplementary Material specifically for patients. Overall, we aim to provide a document that is thorough and accessible for trainees, established providers, and patients.

Stress protocols

Angina can encompass a wide variety of symptoms, ranging from chest, arm, or jaw pain to shortness of breath, nausea, or epigastric discomfort. Angina occurs due to an inadequate supply of blood to the heart, particularly during exercise or stress. Atherosclerosis of the coronary arteries, either in the large epicardial arteries or the microvasculature, is the most common reason for angina. PET MPI is a powerful tool for identifying the location and extent of coronary stenosis. In PET MPI, patients are injected with radioactive tracers which are known to temporarily deposit within myocardial tissue. During stress, either via exercise or a pharmaceutical agent, there will be an imbalanced uptake of the radiotracers in the heart, with less uptake downstream from a significant stenosis. Both qualitatively and quantitatively, clinicians can detect these imbalances of radiotracer to identify areas of heart muscle affected by coronary stenosis.[1,2]

Pharmacological stress testing is the standard in PET MPI, as opposed to single photon emission computed tomography (SPECT) where exercise protocols are preferred (*Figure 1*). Exercise protocols are more challenging in PET MPI due to the short-half-lives of the PET tracers, particularly ^{82}Rb-chloride and ^{15}O-water which have half-lives of 75 s and 2.1 min, respectively.[5,6] These brief half-lives preclude safely moving a patient from either a treadmill or stationary bicycle to the PET scanner after injection of the tracer at peak exercise. Exercise protocols are more feasible with ^{13}N-ammonia and ^{18}F-flurpidaz due to their longer half-lives. However, exercise protocols typically prevent the measurement of myocardial blood flow (MBF) regardless of tracer, as imaging must be performed at the time of tracer injection to capture first-pass myocardial extraction.

Regadenoson, adenosine, and dipyridamole, the available vasodilator stress agents, are adenosine agonists. Areas of myocardium distal to fixed stenoses will have impaired vasodilator response compared with normal vessels, thus causing heterogeneous tracer uptake.

Dobutamine is an adrenergic agonist which increases myocardial oxygen demand via increases in heart rate and contractility. Patients undergoing dobutamine or exercise protocols are expected to achieve 85% of max-predicted heart rate for the test to be considered diagnostic. Atropine, an anticholinergic drug, can be administered if patients have not met max-predicted heart rate despite high doses of dobutamine.[7]

Stress-electrocardiogram (ECG) should be performed with both exercise (treadmill or bicycle) and pharmacologic stress protocols. Stress-ECG may uncover high-risk findings like ischaemic ST changes, such as ST-depressions, or arrhythmia.[8]

Patient preparation

Intake of caffeine, an adenosine antagonist, can interfere with vasodilator agents and therefore caffeine-containing foods, beverages, and medications must be discontinued for at least 12–24 h prior to the exam.[9] Decaffeinated beverages often contain small amounts of caffeine that may interfere with vasodilation and should also be avoided. Failure to adhere to proper preparation may lead to non-diagnostic studies and/or rescheduling of the exam. Patients are also instructed to take nothing by mouth, except water, for at least 4 h prior to the exam.[10] Common foods, beverages, and medications to avoid can be seen in *Figure 2*. Methylxanthine-containing medications, such as theophylline, must also be held for five half-lives before a vasodilator exam.

Referring physicians can consider temporarily discontinuing haemodynamically active drugs, such as calcium-channel blockers, beta-blockers, or vasodilators. For exercise protocols, calcium-channel blockers and beta-blockers may prevent the achievement of maximum predicted heart rate. For vasodilator testing, the decision to hold anti-anginal medications is more controversial. There are mixed data on whether anti-anginal medications, and beta-blockers in particular, attenuate perfusion defects and therefore may reduce the sensitivity of the exam.[11–13] However, discontinuation of chronic medications may result in worsening of underlying tachyarrhythmias and hypertension. The most recent American Society of Nuclear Cardiology procedural guidelines recommend discontinuation of haemodynamically active medications, whereas the European Association of Nuclear Medicine procedural guidelines do not have an explicit recommendation.[7,10]

Decisions on haemodynamically active medications should be tailored to the patient and the indication of the exam. For example, referring physicians may wish to hold anti-anginal medications when trying to

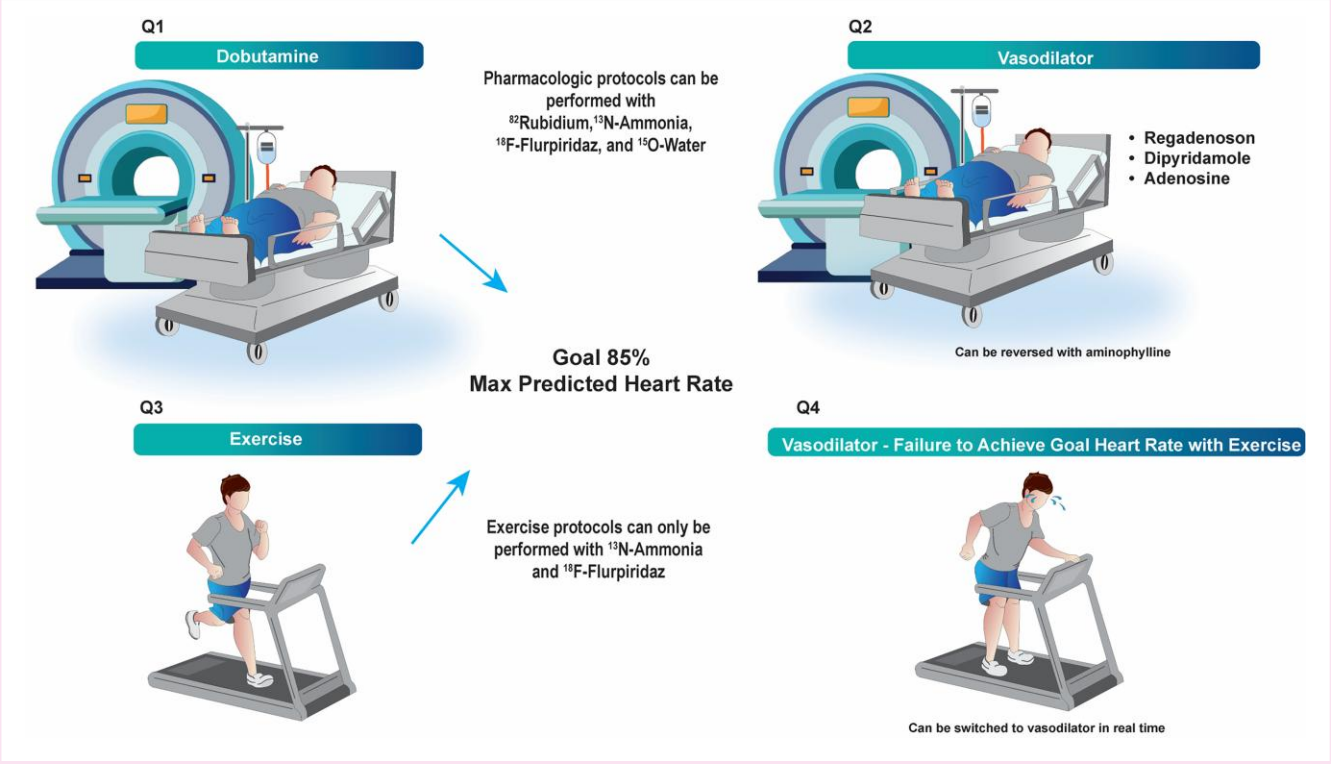

Figure 1 Methods of stress testing. Stress testing can be performed pharmacologically (Q1, Q2, Q4) or with exercise (Q3). Pharmacological stress testing is more common with PET compared with single photon emission CT, the alternative technology to perform nuclear MPI. Patients undergoing vasodilator stress tests may experience side effects such as flushing, headache, shortness of breath, and chest pain. Similarly, dobutamine may cause palpitations, chest pain, headache, flushing, and shortness of breath. Reproduced with permission from Abadie *et al.*[4]

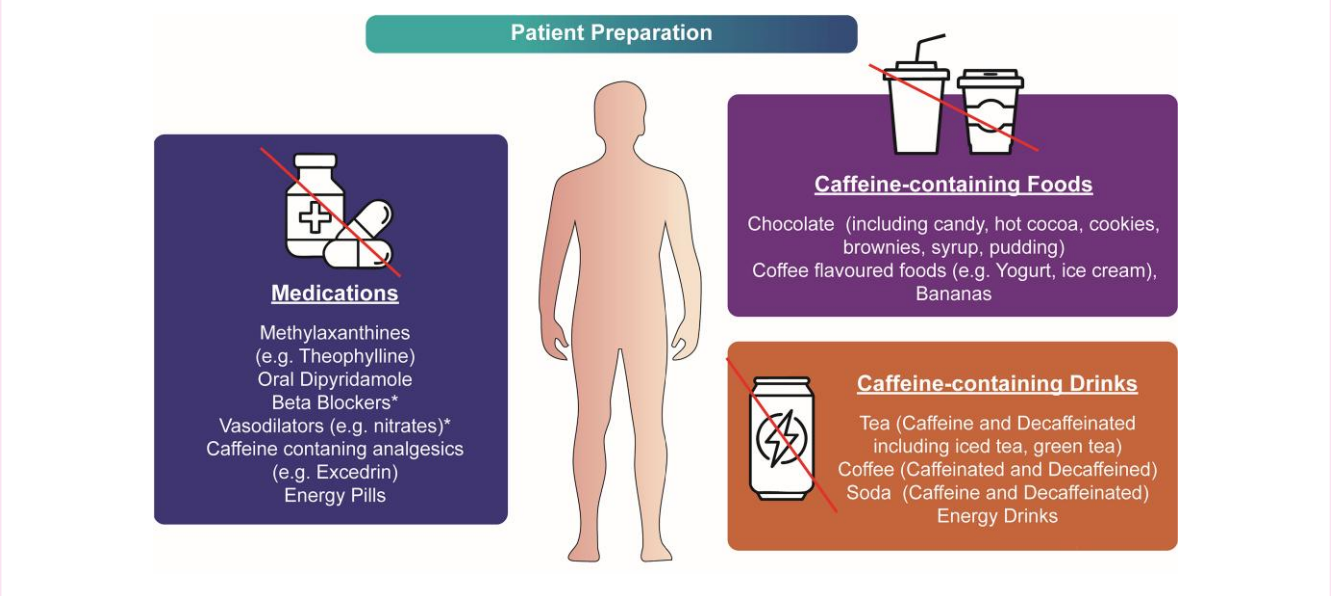

Figure 2 Examples of medications, foods, and drinks that may interfere with image quality. Some providers may continue beta-blockers or vasodilators during exercise testing to assess the degree of ischaemia while on treatment. Reproduced with permission from Abadie *et al.*[4]

diagnose ischaemia in patients without established CAD. Conversely, with exercise protocols, referring physicians may continue anti-anginal medications in patients with established CAD to assess their effects on the relief of symptoms, the reduction of ischaemia, and the amount of myocardium at risk. Beta-blockers can attenuate perfusion heterogeneity in both exercise and pharmacologic protocols but should not have significant effects on quantitative MBF. If haemodynamically active medications are to be interrupted, they should ideally be stopped for three to five half-lives.[13–15]

Patients should be positioned in a supine position in a comfortable manner, with arms above their heads out of the camera's field-of-view. A comfortable position should be ensured with supports below the knees and arms and with appropriate belts. Furthermore, patients should be informed about the common symptoms caused by vasodilators to avoid movement during image acquisition. Common side effects of vasodilators are flushing, headache shortness of breath, and chest pain.[7] Aminophylline, an adenosine receptor antagonist, can be administered to shorten the duration of adverse effects of adenosine receptor agonists after image acquisition.[7] Dobutamine may cause palpitations, chest pain, headache, flushing, and shortness of breath, or exacerbate tachyarrhythmias.

More detailed information regarding patients' preparation, as well as general (contra)indications to cardiac stress tests have been covered in dedicated imaging guidelines, to which the reader is referred.[7,10]

Clinical Pearl #1	One size does not fit all—PET MPI should be tailored to answer the clinical question. For each case, it is important to select the appropriate stress modality (exercise vs. pharmacologic) and decide on whether to withhold haemodynamically active medications.

Imaging protocols

The short-half-lives and high energy of PET tracers simplify imaging protocols. As compared with SPECT protocols, all PET protocols can be performed in 1 day and often in less than an hour. For the tracers with very short-half-lives (^{82}Rb-chloride and ^{15}O-water), the same dose of tracer may be given for both rest and stress imaging, reducing radiation exposure. Imaging must be performed immediately after tracer injection to capture the arterial input function needed to quantify MBF. The interval between rest and stress imaging varies based on which tracer is used; for example, imaging protocols with ^{82}Rb-chloride, with the shortest half-life of 75 s, are typically quicker than those with ^{13}N-ammonia, with a longer half-life of 10 min.[16,17] Examples of protocols with ^{82}Rb-chloride, ^{13}N-ammonia, the newly approved, ^{18}F-flurpiridaz, and ^{15}O-water can be seen in *Figures 3–6*.

Tracers

PET MPI has traditionally been performed using either ^{82}Rb-chloride, ^{13}N-ammonia, or ^{15}O-water.[16,17] ^{18}F-Flurpiridaz was recently approved in the USA.[20] Other F-18-based tracers are in earlier clinical-phase development.[21] A summary of the properties of the current PET perfusion tracers is shown in *Table 1*.

Because of their short physical half-lives, the use of ^{13}N-ammonia and ^{15}O-water require an on-site cyclotron. ^{82}Rb-chloride is produced from an ^{82}Sr/^{82}Rb-generator, with supply typically lasting 4–8 weeks, depending on the initial activity and desired radiotracer activity. ^{18}F-labelled tracers, because of the longer isotope half-life (~2 h), can be produced at regional cyclotron or radiopharmacy and distributed as a unit dose. The short-half-lives of ^{82}Rb-chloride and ^{15}O-water enable fast rest–stress imaging protocols, whereas the use of ^{13}N-ammonia or ^{18}F-flurpiridaz require either a delay of four to five half-lives or a higher dose for the second scan (typically stress). The effective radiation dose (mSv/GBq) is an order of magnitude lower for the short-lived isotopes than for ^{18}F-labelled tracers, which can be balanced by reducing the total injected activity (at the expense of longer imaging times) and/or performing stress-first protocols. ^{82}Rb-chloride has a longer positron range than other perfusion tracers, but this has only limited effects on spatial resolution in daily practice.[16,17]

The physiological properties of perfusion tracers vary in terms of myocardial extraction from blood and tissue retention, which may have an impact on image quality and choice of kinetic model for MBF quantification. ^{15}O-water is a freely diffusible tracer with a high initial tissue extraction over a wide range of MBF values, resulting in a tracer uptake rate (K_1) that is close to the true MBF. However, ^{15}O-water washes out rapidly and there is effectively no tracer retention in the myocardium above the blood background level. Thus, interpretation is based on parametric images of quantitative MBF rather than of qualitative and semi-quantitative retention images. ^{13}N-ammonia, like ^{15}O-water, has high initial tracer extraction along with tissue retention of ~50–60% at peak stress. ^{82}Rb-chloride has substantially lower extraction fraction and tracer retention at peak stress than ^{13}N-ammonia (*Table 1*). The ^{18}F-labelled tracers with available data show high extraction fraction and retention[16,17,23,24] (*Figure 7*).

Incomplete extraction and retention of tracer can reduce the contrast between high- and low-MBF regions, leading to an underestimation of regional perfusion abnormalities when assessed visually. When MBF is quantified, suboptimal extraction is corrected using a tracer-specific equation. The reliance on tracer-specific correction factors in tracers with lower extraction, such as ^{82}Rb-chloride, may have increased variability, particularly at higher blood flow ranges.[16,17] However, these differences are largely negligible in clinical practice.[26,27]

The appropriate tracer for an institution must factor in real-world factors, such as cost, availability, and patient population. ^{13}N-ammonia and ^{15}O-water, for example, require an on-site cyclotron with close interval between production and patient-injection. An on-site cyclotron may not be feasible for many institutions. Alternatively, ^{82}Rb-chloride is created via an ^{82}Rb-generator via the decay of ^{82}Strontium (^{82}Sr); generators are typically placed adjacent to the PET scanner with autoinjectors in the patient. A sufficient volume of PET MPI must be performed to justify the expense of an ^{82}Rb-generator before the end of its lifespan. ^{18}F-Flurpiridaz, the most recently approved PET tracer, has the longest half-life and can be created at a local radiopharmacy and delivered on the day of testing. Lastly, if an institution has a specific population for which exercise testing is critical, ^{13}N-ammonia and ^{18}F-flurpiridaz are the only current options. Each tracer comes with unique benefits and challenges; the optimal tracer will vary from institution to institution.[22,24]

Clinical Pearl #2	Tracer production, half-life, protocols, extraction, and artefacts differ. These factors must be considered on both the patient level (i.e. image interpretation) and institutional level (i.e. setting up a nuclear practice).

Image acquisition

Contemporary PET scanners operate in 3D acquisition mode, as opposed to older 2D systems. Three-dimensional systems are more

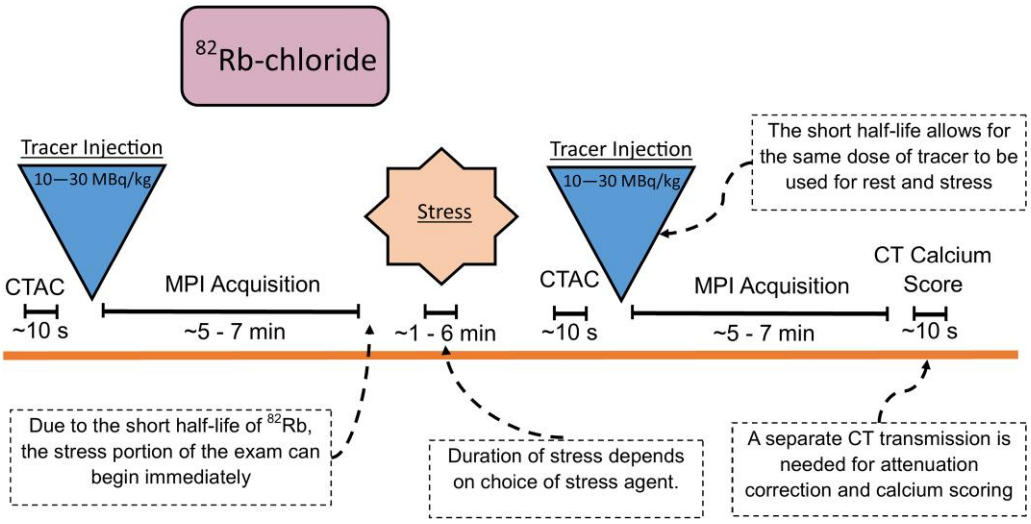

Figure 3 Example protocol with ^{82}Rb-chloride.

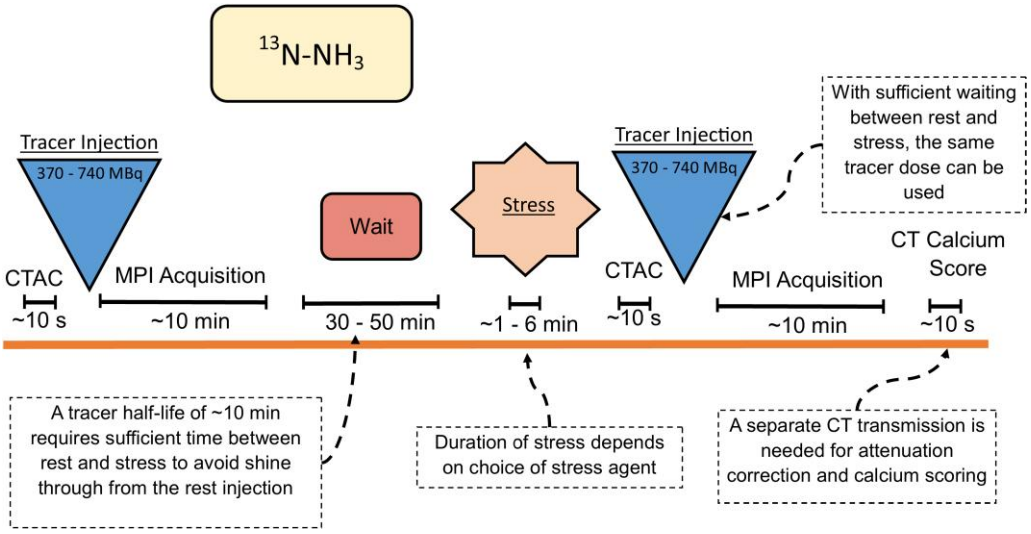

Figure 4 Example protocol with ^{13}N-ammonia (^{13}N-NH$_3$). Protocols with shorter wait times can also be performed, using subtraction techniques to adjust for the residual activity.[18,19]

sensitive, requiring lower injected tracer activity, and therefore, lower patient radiation exposure. Careful consideration should be given to optimizing injected dose to avoid detector saturation during the blood pool first-pass intake (when MBF quantification is acquired), while preserving sufficient activity in the myocardial tracer retention phase is needed for perfusion images.[5,16] Detector saturation may result in falsely elevated MBF due to underestimation of the blood input function. The shorter-lived tracers, ^{82}Rb-chloride and ^{15}O-water, are particularly challenging in this regard. The maximally tolerated activity varies greatly between 3D PET systems. New digital PET systems integrated with silicon photomultiplier detectors have increased the dynamic range of 3D PET systems, potentially reducing the need to trade-off perfusion image quality for MBF accuracy.[5,6,28]

Photons emitted from the heart can be heterogeneously deflected from their linear path by surrounding tissues, reducing count rates at the detector. This phenomenon, called attenuation, can cause attenuation artefacts. PET cameras are commonly combined with computed tomography (CT), allowing for attenuation correction. In addition, hybrid PET/CT systems enable the combination of MPI with coronary artery calcium assessment, and, with scanners containing ≥64 CT detector rows, coronary CT angiography.[29–31] The use of state-of-the-art methodology enables integration of CT and PET imaging with an acceptable radiation exposure to the patient; the addition of a non-contrast CT scan also allows for non-obstructive, as well as obstructive plaque, to be detected via the detection of coronary calcium.

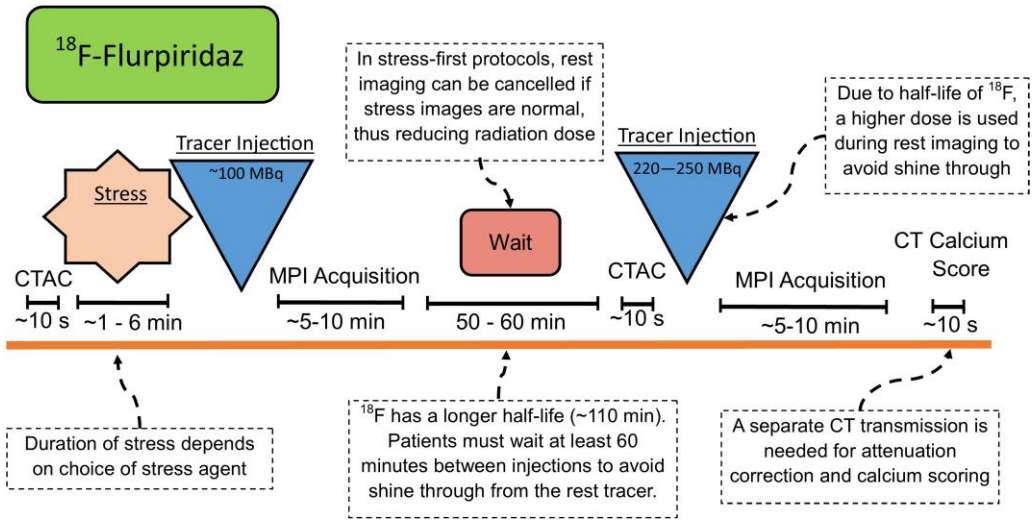

Figure 5 Example protocol with ^{18}F-flurpiridaz. Stress-first imaging is preferred, as normal stress perfusion obviates the need for rest imaging. This may reduce radiation exposure, which is particularly important for ^{18}F-flurpiridaz given its higher radiation dose compared with ^{13}N-ammonia and ^{82}Rb-chloride. Rest-first protocols are also feasible/acceptable. Protocols with shorter wait times can be performed, using subtraction techniques to adjust for the residual activity, although these techniques have not specifically been validated with ^{18}F-flurpiridaz.[18,19]

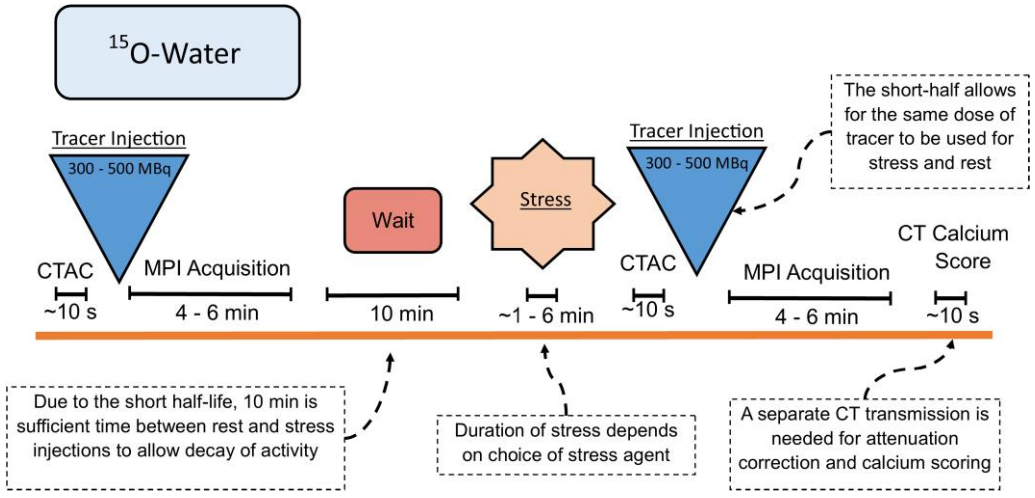

Figure 6 Example of protocol with ^{15}O-water.

Image reconstruction

Similar to SPECT imaging displays, analytic reconstruction (typically with filtered back projection) and iterative reconstruction are the two techniques used for PET image reconstruction. Early cardiac PET imaging used analytical approaches for image reconstruction due to the excessive computing time required for iterative algorithms. As a result of significant improvements in computing technology and more efficient iterative algorithms, iterative reconstruction now is widely available and is the standard for PET image reconstruction.

In iterative reconstruction, the fundamental concept is to make a guess about the location of activity distribution. The projection data produced by this activity distribution are calculated and compared with the actual data acquired. If the two data sets differ, then the guess is adjusted based on the difference and the entire process is repeated. This process repeats until the data sets match. The crucial components of iterative reconstruction are the method(s) used to update the estimated activity distribution based on the differences in data sets and the calculation of projection data from the estimated activity distribution. The most commonly used approach in iterative reconstruction is the maximum-likelihood expectation maximization (MLEM) algorithm. MLEM requires much iteration to generate a clinically reasonable image and is computationally demanding.[32] A modification to the MLEM algorithm, ordered subset expectation maximization (OSEM), allows for

Table 1 Tracer properties for PET MPI

	^{82}Rb-chloride	^{13}N-ammonia	^{15}O-water	^{18}F-tracers[a]
Isotope production method	Generator	Cyclotron	Cyclotron	Cyclotron
Isotope half-life (min)	1.3	10	2.0	110
Mean estimated positron range (mm)[b]	6.8	1.8	3.0	0.6
Effective dose (mSv/GBq)	1	2	1	≈20
Peak stress/rest extraction (%)[c]	35/70	95/100	100	95/100
Peak stress/rest retention (%)[c]	25/70	50/90	0	55/90
Dose range/typical dose	10–30 MBq/kg	370–740 MBq	300–500 MBq[d]	≈100/220–250 MBq[e]

[a]Currently data for ^{18}F-flurpiridaz and preliminarily data for ^{18}F-SYN2 available.[16,22]
[b]Data from Conti and Eriksson[22].
[c]Data from Murthy *et al.*[16]
[d]Three-dimensional scanner.
[e]Rest/stress.

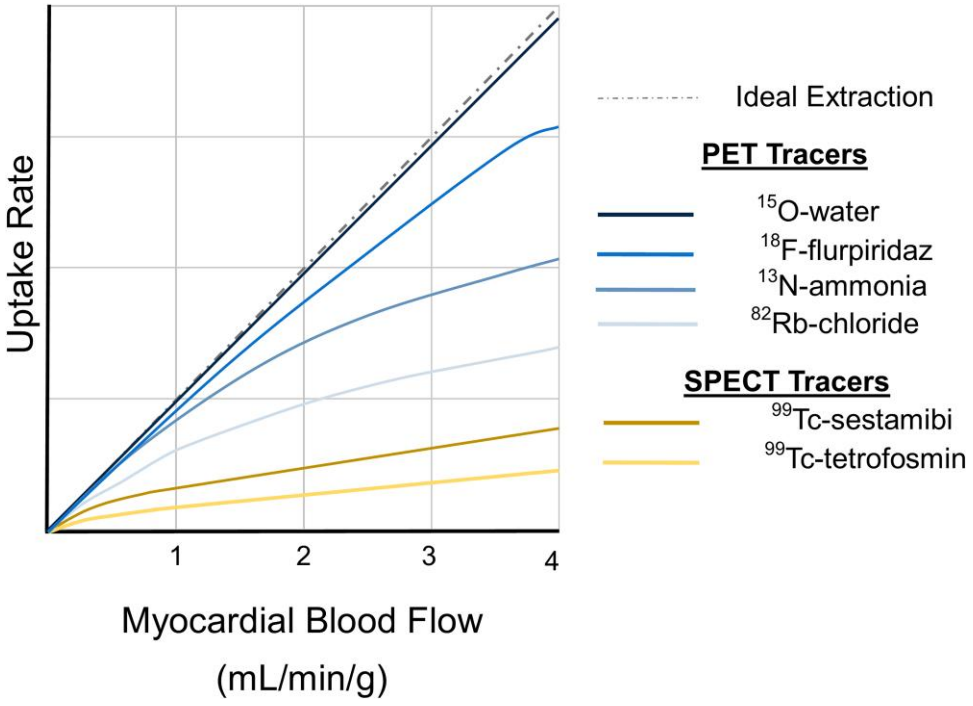

Figure 7 Comparison of myocardial extraction between different commercially available PET and SPECT tracers.[25]

iterative construction to be clinically feasible. In OSEM, the full data set is not needed to update the image estimate. Rather, data from a few projections (subsets) are used to perform updates, thereby significantly decreasing computation time.[33]

The advantage of iterative reconstruction over filtered back projection (analytic approaches) is the incorporation of many characteristics of the data acquisition, including attenuation, scatter, randoms, spatial resolution, and dead time, into the reconstruction model. This allows for the camera acquisition process to be more accurately represented in the data and yields higher fidelity images. Generally, a higher number of iterations results in more accurate image estimates with the trade-off of increased noise. Noise can be reduced by post-reconstruction smoothing (*Figure 8*). Most of the iterative reconstruction challenges encountered in the early days of clinical PET adoption have been resolved with modern computational advances. Images can now be reconstructed and displayed in <1–2 min.

Imaging display and interpretation

Interpretation of PET-MPI studies should integrate all available clinical data including patient history, stress testing haemodynamics, electrocardiographic data, qualitative and semi-quantitative myocardial perfusion, gated left and right ventricular size and function, quantitative MBF, and CT findings, in particular the presence or absence of coronary artery calcifications with or without dedicated coronary artery calcium scoring (*Figure 9*). There are several commercially available software packages that allow for the display and interpretation of these data

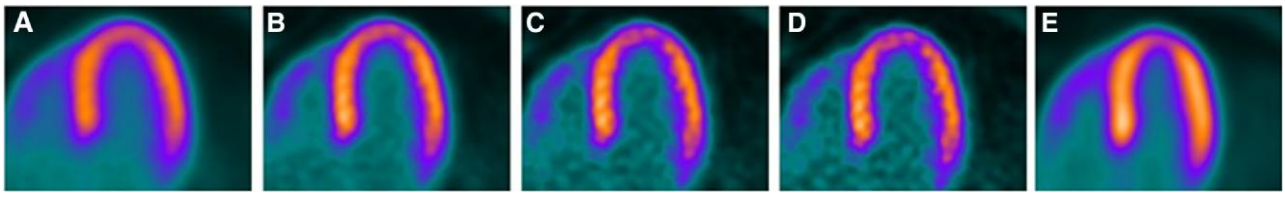

Figure 8 Iterative reconstruction and filtering. Cardiac PET horizontal long axis images reconstructed using OSEM algorithm. (*A*) 1 iteration, 5 subsets; (*B*) 3 iterations, 5 subsets; (*C*) 7 iterations, 5 subsets; (*D*) 10 iterations, 5 subsets; (*E*) 3 iterations, 5 subsets with an 8 mm Gaussian smoothing filter.

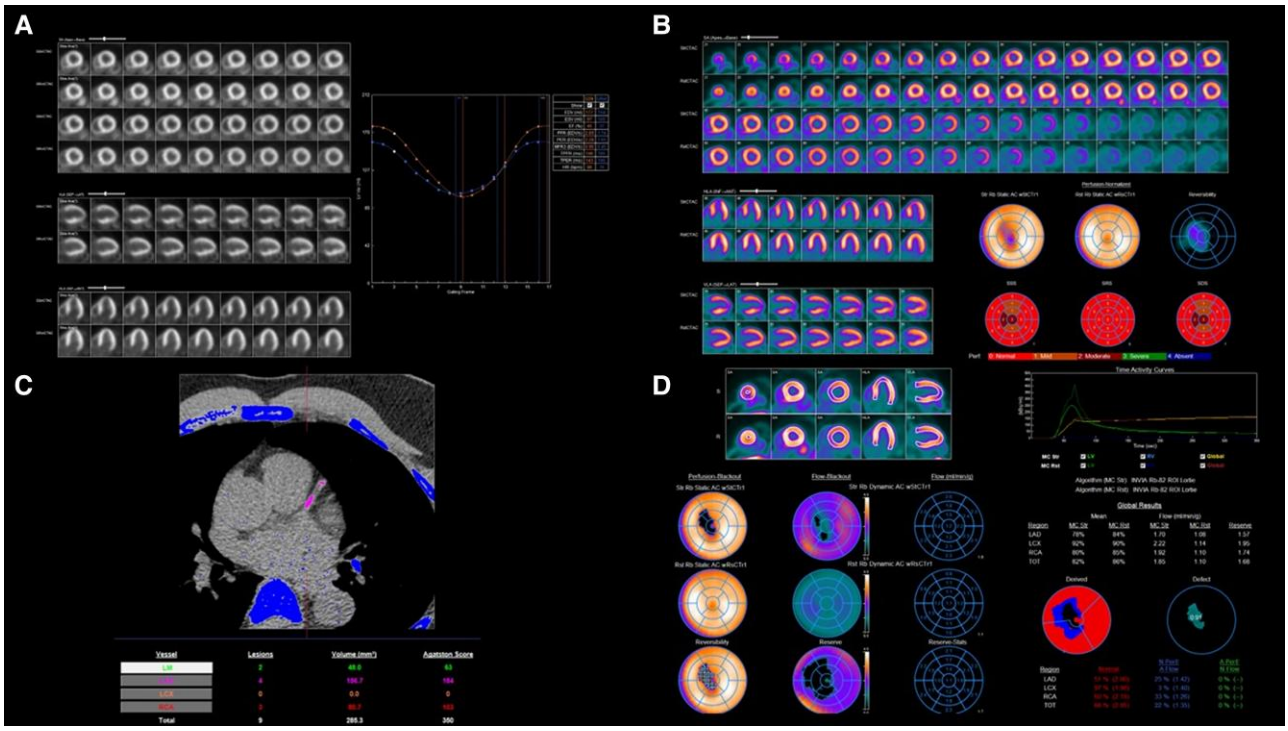

Figure 9 Elements of a cardiac PET myocardial perfusion study. (*A*) Gated images at stress (top row) and rest (bottom row) with quantitative analysis of left ventricular ejection fraction and volumes. (*B*) Static perfusion images at stress (top row) and rest (bottom row) displayed in short axis, horizontal long axis, and vertical long axis planes. Perfusion defects are scored using a semi-quantitative scale on a bulls-eye plot, with summed stress, summed rest, and summed difference scores. (*C*) Coronary artery calcium score. (*D*) MBF analysis using tracer kinetic modelling, reporting rest, stress, and reserve MBF. ^{82}Rb-chloride is the tracer used in this study.

and allow for quantitative analysis of MPI studies.[34,35] Additionally, it is recommended that PET-MPI reports contain structured data elements, as previously described in American Society of Nuclear Cardiology (ASNC) guidelines and European Association of Cardiovascular Imaging (EACVI) position papers.[36–38]

MPI data are displayed in standard tomographic planes: short axis, vertical long axis, and horizontal long axis (*Figure 10*). From these views, the left ventricle can be displayed in a 17-segment model or polar map, colloquially known as a bull's eye. The polar maps are able to communicate the size, severity, and anatomical distribution of a defect[39] (*Figure 11*, *Table 2*). In this system, scores of 0 through 4 correspond to normal, mildly abnormal, moderately abnormal, severely abnormal, and absent uptake of radiopharmaceutical, respectively, in a particular left ventricular segment. Perfusion defects can be reported as fixed (present on rest and stress imaging) or reversible (only present on stress). Reversible defects typically represent ischaemia; fixed defects could represent scar or hibernating myocardium.

The total perfusion score at rest is the summed rest score (SRS), at stress is the summed stress score (SSS), and the difference between rest and stress, the summed difference score (SDS). The percentage of myocardium at risk can be calculated by dividing the SSS or SDS by 68 and multiplying by 100.[39]

Left ventricular ejection fraction and left ventricular end diastolic and end systolic volumes can be accurately calculated by commercially available software using the gated images with 8 or 16 frames/cardiac cycle. Ejection fraction and left ventricular volumes should be reported for

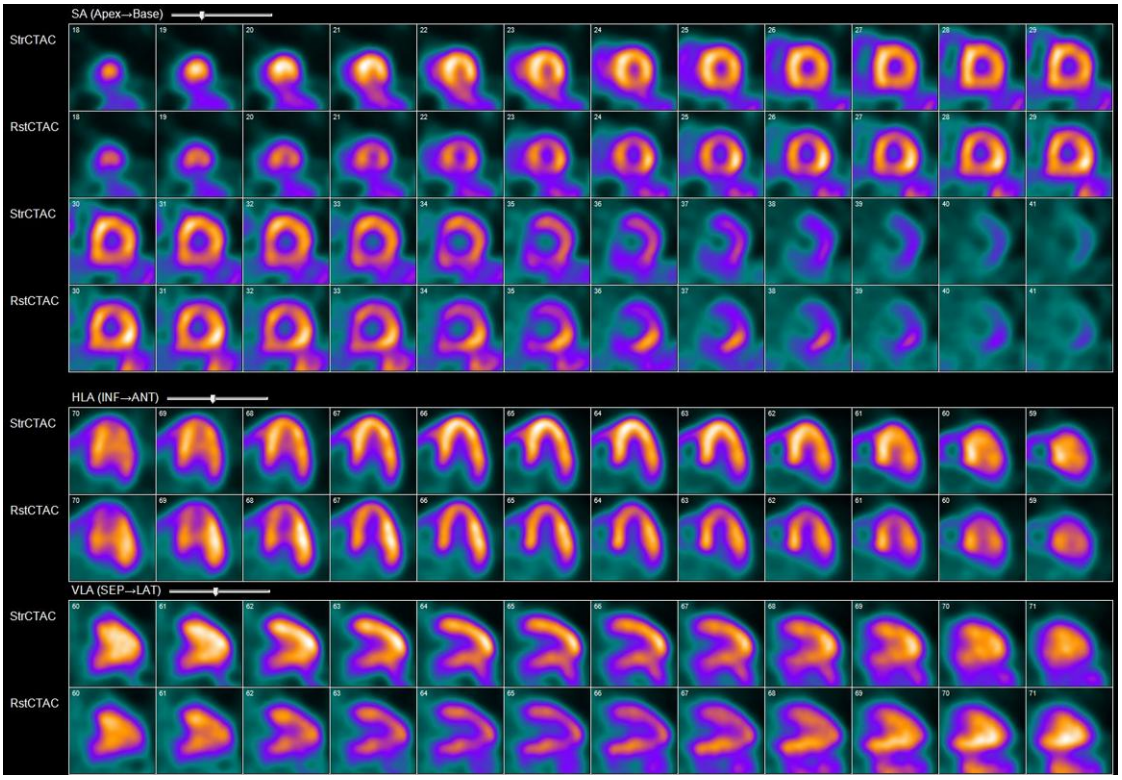

Figure 10 Standard views of the left ventricle. Traditionally, stress images are placed above rest images. SA, short axis that runs from the apex (left) to the base (right); HLA, horizontal long axis that runs from the inferior (left) to anterior wall (right), VLA, vertical long axis that runs from the septum (left) to the lateral wall (right).

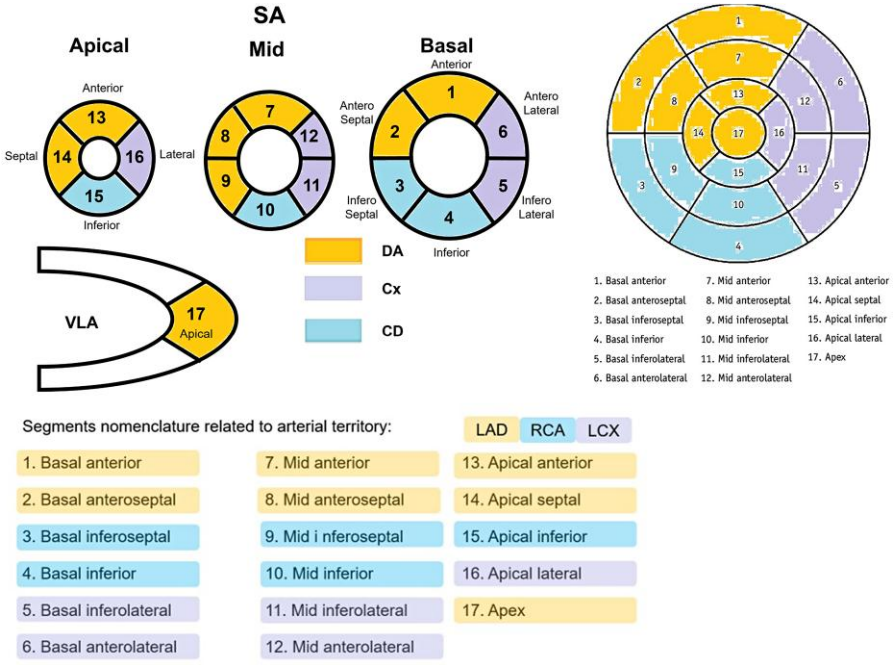

Figure 11 Standard 17-segment model and polar map for reporting semi-quantitative perfusion. Each segment corresponds to a particular vascular distribution. Reproduced with permission from Abadie *et al.*[4]

Table 2 Criteria for semi-quantitative assessment of defect size

Summed score	≤3	Normal or equivocal
	4–8	Mild defect
	9–12	Moderate defect
	>12	Severe defect

Table 3 Categories of left ventricular function by ejection fraction

Categories of left ventricular function	Ejection fraction (%)
Hyperdynamic	≥70
Normal	55–70
Low normal	50–55
Mildly	45–50
Moderately	35–45
Severely reduced	≤35

both rest and stress imaging data[40–42] (*Table 3*). Dyssynchrony, such as in the setting of left bundle branch blocks or ventricular pacing, can also be assessed qualitatively and quantitatively (*Figure 12*).

Quantitative MBF analysis is a central component of PET MPI studies and should be reported whenever available. Validated kinetic models used to calculate MBF are available in commercially available software, making MBF analysis clinically feasible, accurate, and reproducible.[16,37,43] Rest MBF and stress MBF, in addition to MBF reserve (MFR, the ratio of stress MBF to rest MBF), should be included in PET MPI reports and integrated into the overall interpretation of the PET-MPI study. Quantitative MBF data should be additive to the relative myocardial perfusion and left ventricular functional data and should factor into the overall impression of the PET-MPI study (*Figure 13*). The most commonly used threshold for an abnormal MFR is <2.0.[44] Of note, however, different stress modalities augment MBF differently, with exercise typically a two-fold increase, and vasodilators a three- to four-fold increase; dobutamine can augment greater than vasodilator agents.[45]

Quantitative MBF has shown good agreement with invasive measures of stenosis severity, such as fractional flow reserve, and therefore may be able to predict the need for revascularization.[46] Quantitative MBF is particularly helpful in cases where the relative myocardial perfusion images are normal with abnormal myocardial flow reserve. In such cases, the first step is to ensure that there are no technical factors to account for this discordance (*Figure 11*). Assuming there are no other causes for abnormal MFR (for example, lack of vasodilator response, low MFR due to high resting MBF, technical issues with dynamic image acquisition), one needs to consider multi-vessel obstructive coronary artery disease and/or coronary microvascular dysfunction among other causes as possible aetiologies for low MFR[44] (*Figure 14*). Because perfusion imaging relies on the heterogeneous uptake of radiotracer in the left ventricle, severe obstruction in all coronary vessels may be missed, a phenomenon called balanced ischaemia. Quantitative MBF increases the sensitivity of PET in this high-risk population. Acknowledging the presence or absence of coronary artery calcium, the presence or absence of left ventricular systolic dysfunction, a decrement in left ventricular systolic function at the time of stress, and clinical history can assist in providing an assessment to why there are abnormalities in MFR despite visually normal perfusion.

Clinical Pearl #3	The ability to quantify myocardial blood flow is a key advantage of PET MRI compared with traditional SPECT imaging and should be readily incorporated into reading and reporting protocols.

Artefacts and non-diagnostic studies

High-quality scans and precise image interpretation are crucial for fully leveraging the capabilities of cardiac PET in patient care. Imagers should be able to distinguish between low and high-quality PET-MPI scans, identify reasons for non-diagnostic studies, understand what causes these artefacts, and how to effectively correct them.[47] Artefacts are the most frequent reason for non-diagnostic PET-MPI studies, followed by non-response to pharmacological stressors.

Discrepancies between visual interpretation and quantitative flow occur. With vasodilator protocols, when perfusion is normal, stress, and reserve flows are abnormal, it is vitally important to ensure that the patient had an adequate response to the vasodilator. Common reasons for an inadequate response are consumption of adenosine antagonists prior to the examination (e.g. caffeine-containing food and drink) or extravasation of the vasodilating agents. Patients adequately exposed to vasodilators should have an increase in their heart rate and a drop in blood pressure; however, haemodynamic changes are not always reliable. Splenic switch-off, the relative decrease in tracer activity in the spleen during stress compared with rest, can be used to demonstrate that a patient had an adequate vasodilatory response[48] (*Figure 15*). This finding was first described with adenosine protocols, but has more recently been demonstrated with regadenoson.[49] A change in quantitative MBF from rest to stress can also be used to ensure the patient was adequately stressed. Abnormal visual perfusion with normal quantitative flow can also occur.

Common artefacts, independent of radiotracers and vasodilators, include attenuation-correction-artefacts, mis-registration of emission and transmission scans, and patient motion; these artefacts can often be easily recognized and, to a certain extent, improved in post-processing.[50,51] Left ventricular hypertrophy, particularly in hypertrophic cardiomyopathy, can cause an increase in tracer uptake, which can cause the relative difference in the contralateral segments to be mistaken for hypoperfusion.

Quantitative PET-MPI artefacts affecting or rendering MBF assessment uninterpretable often arise from inaccurate attenuation correction, patient movement, and suboptimal tracer-bolus delivery.[17,52] Suboptimal tracer-bolus delivery can be detected via abnormalities in the myocardial time-activity curves[53] (*Figure 16*). Importantly, for both qualitative and quantitative analysis, reduced image count density, for example due to extravasation, use of i.v. ports located close to the heart, or extreme obesity (without injected dose adjustment), can directly affect the diagnostic quality of the study.[50]

Careful scheduling of the scan based on patient characteristics and radiotracer availability, coaching the patients prior to and during the examination, careful review of the fused images, and the use of modern software that enables correction of cardiorespiratory motion and myocardial creep (stress-induced, non-periodical repositioning of the heart in the mediastinum) are critical to mitigate artefacts and minimize

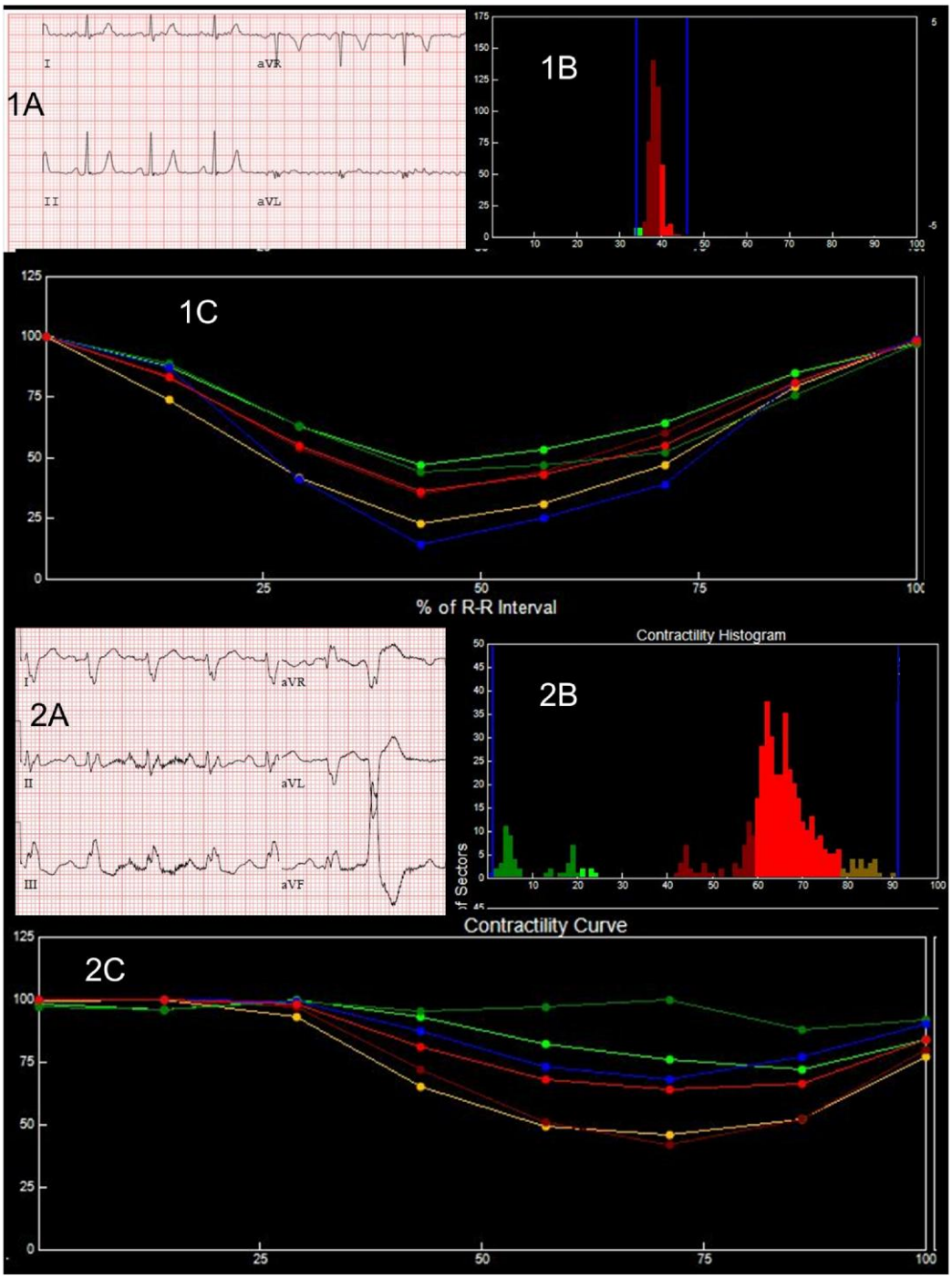

Figure 12 Myocardial dyssynchrony can be accessed via gated PET images. (1*A*) The patient has a narrow QRS on electrocardiogram with a narrow range of R-R intervals (1*B*). Panel 1*C* demonstrates that all the myocardial segments are reaching peak displacement at the same time. Conversely, patient B has a left bundle branch block and premature ventricular contraction (2*A*) with a wide range of R-R intervals (2*B*). Panel 2*C* shows a delayed and dyssynchronous peak displacement of the myocardial segments.

non-diagnostic studies.[47,54–56] *Table 4* summarizes the most frequent artefacts with suggested solutions and *Figure 17* demonstrates examples commonly encountered in clinical practice.

In addition to those general pitfalls, the different radiotracers used in PET MPI might be presented with specific artefacts. ^{82}Rb-chloride, with its rapid decay, might cause detector saturation during tracer first-pass, while ^{82}Sr generator age-related decrease in activity per volume might impact the blood first-pass curve.[57,58] Gastrointestinal tract uptake of the tracer, particularly in patients taking proton pump inhibitors and following gastric bypass surgery, and increased blood pool activity,

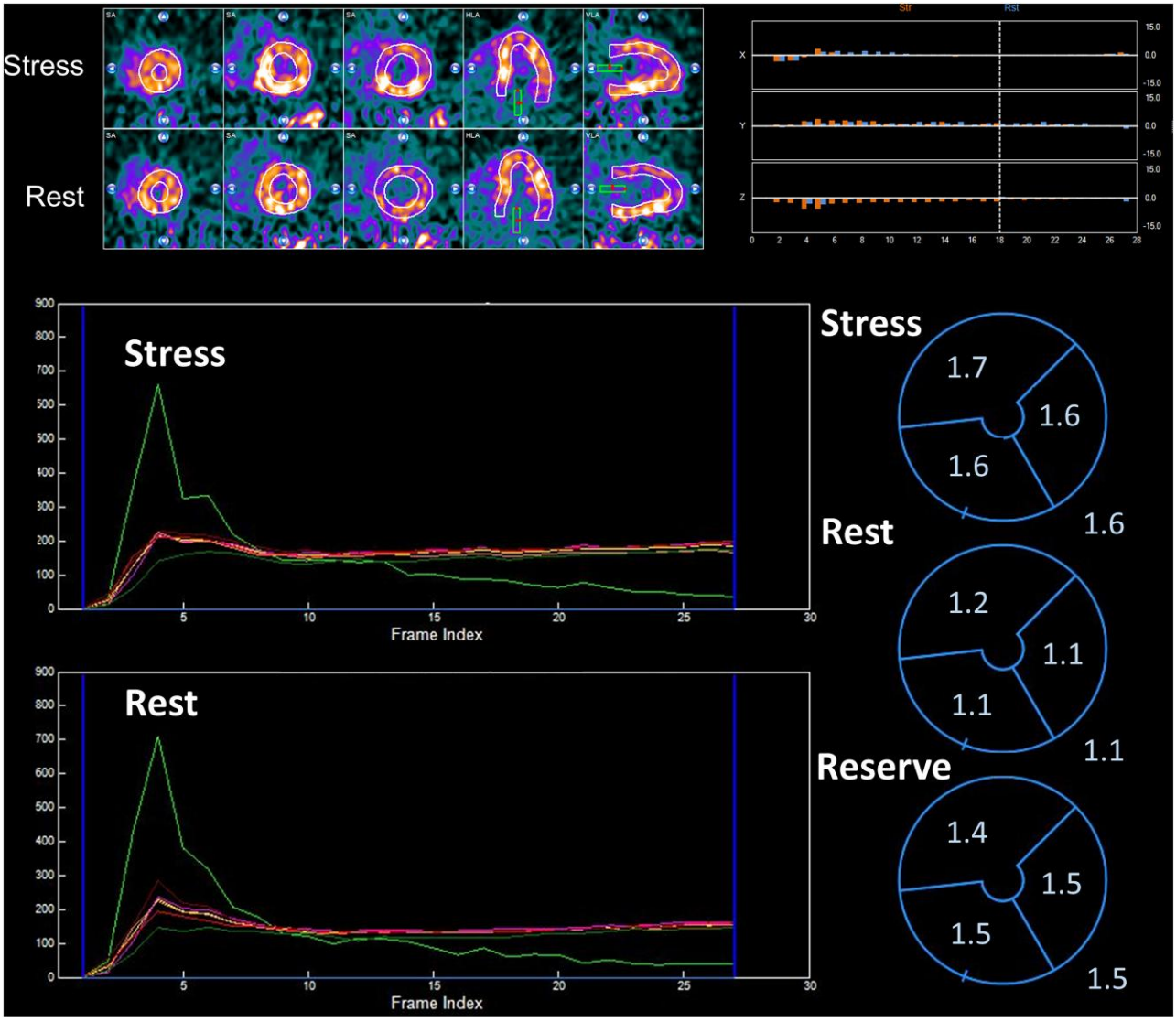

Figure 13 Example of quantitative MBF. Top left: retention images are used to ensure the myocardial border is properly registered and aligns with tracer uptake. Top right: figure demonstrates degree of patient motion during the exam which may interfere with accuracy of blood flow data. Bottom left: time-activity curves showing MBF at stress and rest. Note the early blood pool peak (green) that quickly drops to lower levels of activity. Conversely, the myocardial flow persists throughout the curve (other colours). Bottom right: resultant stress, rest, and reserve flow by vascular distribution, with adjacent global value. ^{82}Rb-chloride is the tracer used in this study.

commonly seen in patients with severely depressed left ventricular function, may limit diagnostic image quality.[59,60]

^{13}N-ammonia, while generally offering high-quality uptake images, is challenged by attenuation artefacts from respiratory movements, such as lung uptake impacting proper visualization of the lateral segments of the left ventricle, myocardial creep, and apical thinning.[17,61–63] The latter is observed with all tracers but is in general more pronounced with ^{13}N-ammonia. A fixed basal lateral/inferolateral wall perfusion defect with normal wall motion and wall thickening can be also observed.[64–66] Finally, increased lung uptake (primarily in rest and less under stress) has been reported in patients with decompensated heart failure, inflammatory lung disease, and recent smoking just prior to the exam.[67,68]

^{15}O-water PET is less susceptible to myocardial creep due to the absence of uptake images; however, it requires meticulous correction for high activity in the blood pool and spill over from the left and right ventricles, a process typically integrated into kinetic modelling software.[69,70]

Clinical Pearl #4	Diagnostic confidence can only be as high as test quality. Ensure you are attempting to pre-empt The introduction of artefacts into images, as well as properly recognizing and reporting them when they occur.

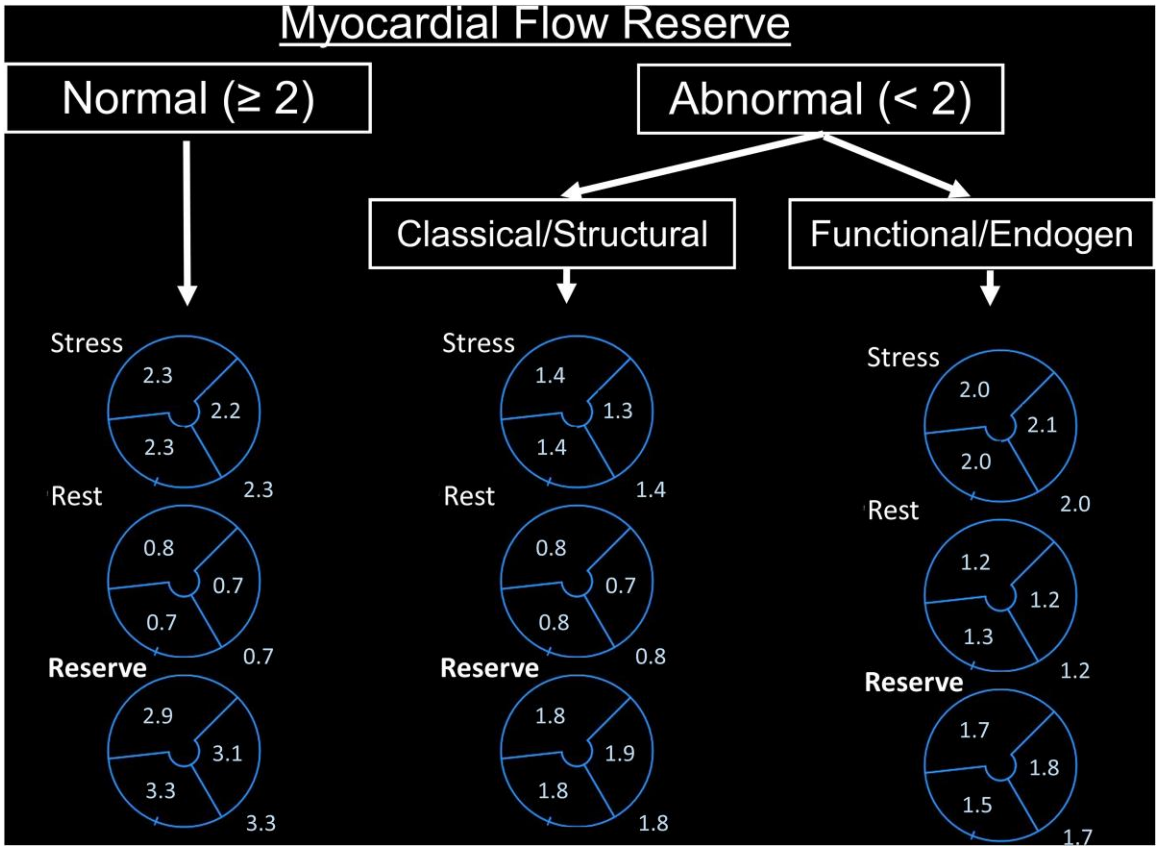

Figure 14 Normal myocardial flow reserve is typically defined as ≥2.0. In the absence of obstructive epicardial disease, an abnormal myocardial flow reserve (<2.0) can indicate microvascular dysfunction. Two main categories of microvascular dysfunction have been described, classical/structural with low stress flow, and functional/endogen with high rest flow.

Viability imaging

Viable myocardium encompasses a broad spectrum of conditions and includes stunned and hibernating myocardium[71] (*Figure 18*). The primary focus of this section will be the detection of hibernating myocardium, which is often indistinguishable from scar on traditional perfusion imaging.[72–74] Viability imaging can identify dysfunctional myocardium that has the potential for recovery with revascularization and can therefore guide therapy.[75]

Viability imaging can be performed with both SPECT, with thallium or technetium (^{99m}Tc), and PET, with ^{18}F-fluorodeoxyglucose (FDG). Delayed thallium imaging is an outdated and rarely used method to assess viability and will not be discussed in this position paper. ^{99m}Tc tracers passively diffuse across membranes where uptake and mitochondrial retention are conditioned by the electrochemical gradient. To assess viability, acquisition of rest images is performed under maximal vasodilatation with nitrates.[9]

PET imaging with FDG is preferred over SPECT for the assessment of viability.[67] FDG has a relatively short-half-life of 109.8 min, or slightly <2 h. Nevertheless, this half-life is sufficiently long to allow shipping of the tracer to remote PET scanning facilities where it cannot be produced with a local cyclotron. Common tracer doses and imaging protocols can be found in *Table 5* and *Figure 19*.

In chronically ischaemic myocardium, there is a relative increase in glucose utilization compared with long-chain fatty acids. Areas of myocardium with resting hypoperfusion on traditional perfusion imaging, but with the uptake of FDG, are considered viable/hibernating (*Figure 19*). The assessment of viability with FDG-PET requires careful patient preparation to promote glucose utilization by the myocardium.

Viability imaging—patient preparation and imaging protocols

To ensure that the myocardium will preferentially use glucose instead of fatty acids, a strict preparation is required. The evening preceding the investigation, a low-fat meal should be consumed. Prior to the exam, non-diabetic patients typically receive a glucose load along with intravenous insulin to promote myocardial metabolism of glucose over fatty acids.[79] This can be achieved via oral glucose loading or a glucose infusion.

Oral glucose loading can be achieved with 25–100 g glucose dose, typically followed by intravenous insulin. The dose of intravenous insulin varies based on the blood glucose level. Studies have demonstrated that with proper protocols and monitoring, the administration of IV insulin has an excellent safety profile.[80] Oral glucose loading is less labour intensive and time consuming, but can result in suboptimal images and up to 10% uninterpretable scans. In diabetic patients, this method will not lead to sufficient cardiac FDG uptake.[81]

With euglycaemic hyperinsulinaemia clamping, there is continuous and simultaneous infusion of glucose and insulin preceding, during,

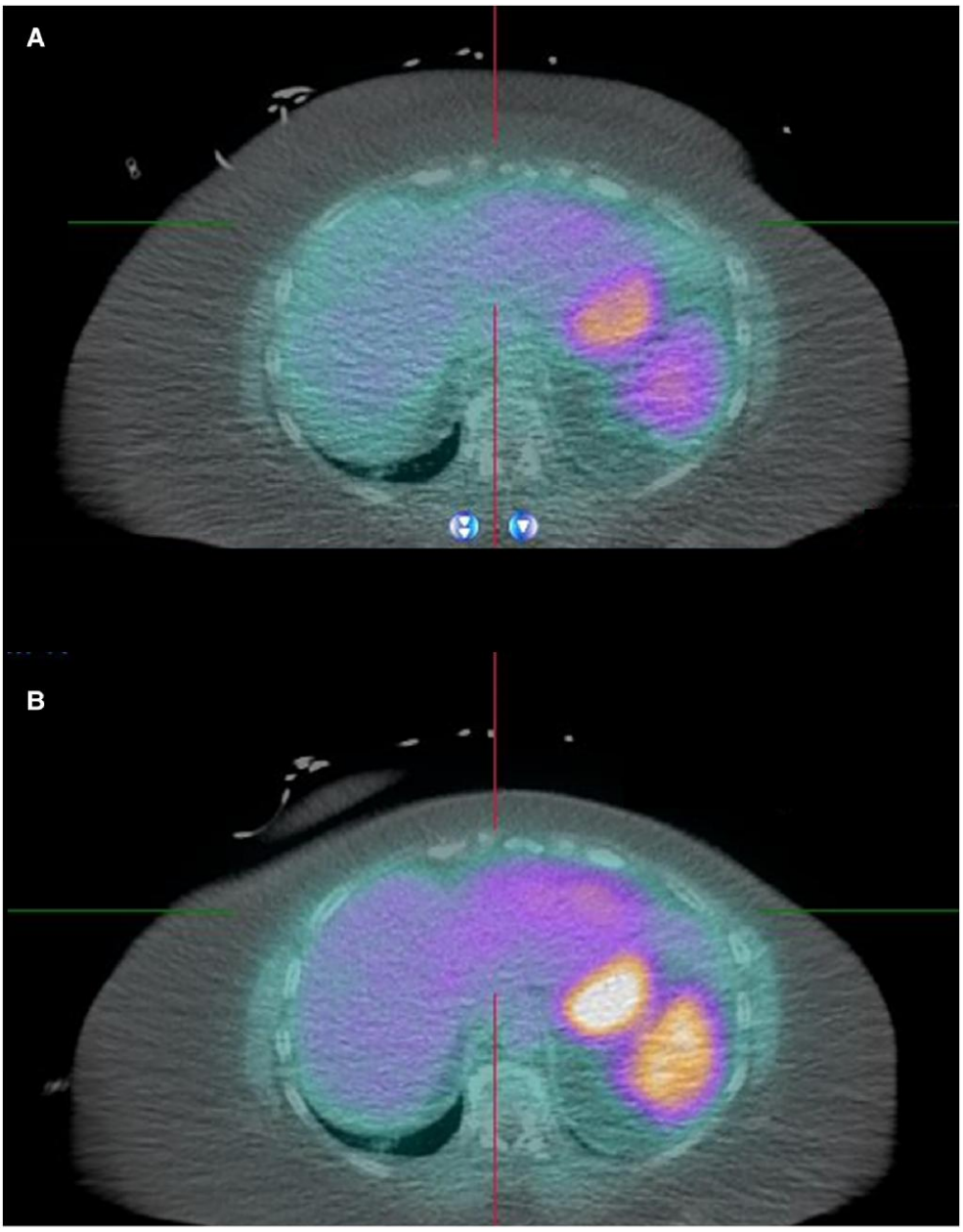

Figure 15 The PET/CT fusion images at stress (*A*) show a decrease in tracer uptake in the spleen compared with the rest images (*B*). This sign, termed splenic switch-off, can be used to ensure the patient had an adequate response to the vasodilator stress agent, which in this case was regadenoson. ^{82}Rb-chloride is the tracer used in this study.

and after FDG administration. This method maximizes glucose, and thus FDG, uptake in the myocardium. This method results in high insulin levels and consequently excellent image quality. However, it can be labour intensive and time consuming. Less extensive versions of this method have also been reported with excellent image quality.[81]

Acipimox, a niacin derivative, can be used to lower free circulating fatty acid levels and thereby promote the use of glucose by the myocardium. Several protocols exist for the use of acipimox and the timing of its administration prior to tracer injection. In these protocols, imaging is started 45–60 min after FDG injection. Flushing, a common side effect of acipimox, can be prevented by orally administering 500 mg acetylsalicylic acid (aspirin). In diabetic patients, a short acting insulin can be added shortly before FDG administration.[81]

Viability imaging—image display and interpretation

FDG-imaging should be interpreted in the context of the resting, and when appropriate, stress perfusion imaging. In cases with hibernation, there will typically be a fixed perfusion defect on the rest MPI imaging with corresponding areas of FDG uptake (*Figure 20*). Conversely, in cases with scar, there will be no FDG uptake in the areas of fixed

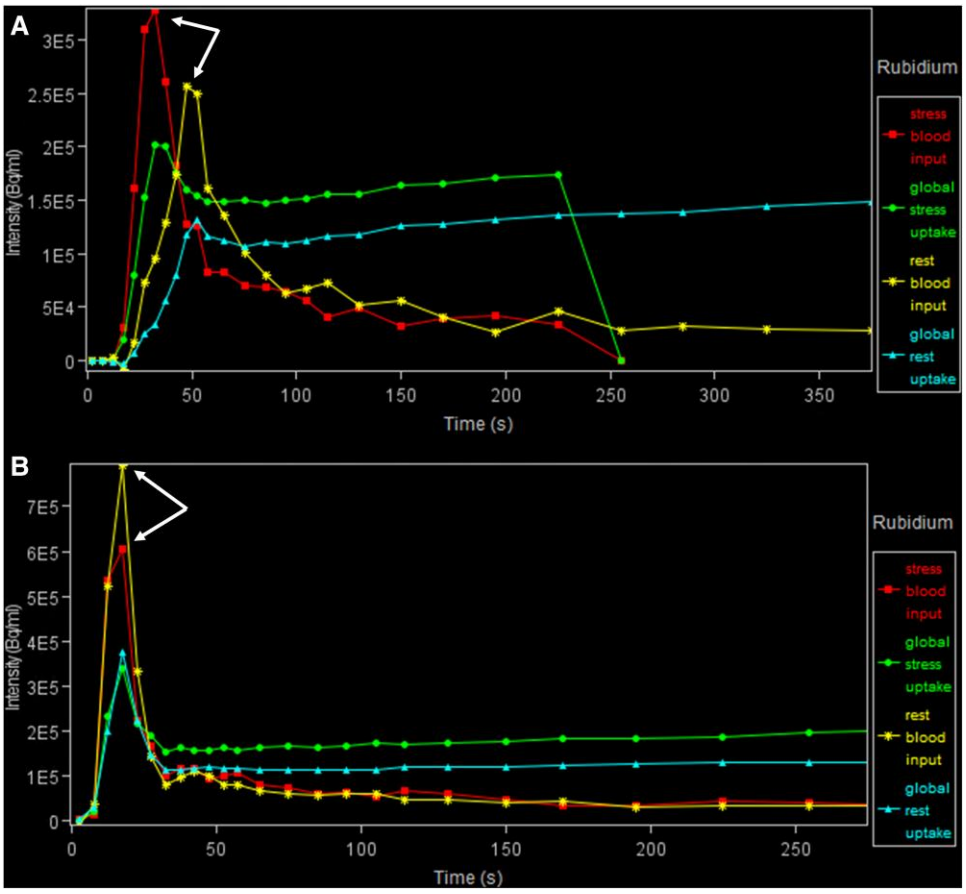

Figure 16 (*A*) The patient had a poorly functioning intravenous catheter and extravasation of the radiotracer. As a result, the curves showing the uptake of the tracer at rest (yellow and blue) are delayed compared with stress (red and green). (*B*) Correct time-activity curve where the rest and stress tracer activity peaks at the same time.

Table 4 Summary of the most common PET-MPI artefacts, how they can be recognized, and potential strategies for mitigating their impact

Artefact	Cause	How to Recognize	How to Tackle
Motion artefacts	• Patient movement or heavy breathing.	• Blurring of images, observed on static and/or dynamic images. • Atypical fixed or reversible perfusion defects (butterfly appearance). • Erroneous myocardial blood flow estimates. • Most prominent usually during stress.	• Patients must stay as still as possible during the scan. • Coaching patients prior to the scan. • Instruct patients during the scan. • Challenging to correct post-acquisition. • Deleting frames with motion and re-summation of motion-free frames might helpful if artefact limited. • Use software that corrects for motion during post-processing.

Continued

Table 4 ***Continued***

Artefact	Cause	How to Recognize	How to Tackle
Attenuation artefacts	• Improper alignment/superimposition of PET and attenuation-correction CT scans. • Commonly during co-registration of transmission and emission scans at the scanner console. • Patient motion/breathing during transmission or emission scans.	• Might be challenging to identify. • Fixed or reversible defect commonly in the lateral (anterior and/or inferior) wall. • Discordance between static and dynamic (motion and breathing-corrected) images.	• Training/feedback of technicians is paramount. • Quality control of fused images at interpretation workstation. • Repeat fusion and reconstruction of images. • Less important if only at rest and in the case of normal stress perfusion.
Suboptimal bolus delivery/ detector saturation	• Improper manual tracer administration. • High-dose injections of short-half-life and low extraction fraction tracers (commonly ^{82}Rb-chloride). • Risk greater in higher sensitivity 3D PET scanners and systems with photomultiplier tube technology.	• Careful examination of the time-activity curves. • Sharp peaks or troughs in the time-activity curve, suggesting rapid changes in tracer concentration. • Plateau-like peaks occurring at the first-pass of the tracer-bolus • Sudden drops in detected counts during the first-pass phase, leading to gaps or incomplete data. • Erroneous myocardial blood flow estimates (usually increased MBF values).	• Optimize injection protocols to ensure smooth and consistent tracer delivery. • Avoid manual injection of tracer. • Use fast-controlled automated tracer injection. • Ensure image acquisition at least 5 s prior to radiotracer injection. • Adjust the tracer dose or optimize the scanner settings to prevent overload of the detection system.
Injection site artefacts	• Tracer injection by port or central venous line near the heart • Local issues with tracer administration (i.v. line).	• High tracer uptake at non-target sites visible on the scan, usually near the injection site.	• Ensure proper injection techniques and inspect the injection site before scanning. • If possible, avoid using central venous lines.
Myocardial creep	• Shift in the position of the heart over the course of a dynamic scan, particularly during stress.	• Visual mis-registration of at least one third of the left ventricular wall width, commonly (but not limited) in the downward (inferior) direction.	• Monitor dynamic dataset frame by frame and correct for any shifts using real-time imaging feedback and post-processing alignment tools.
Spillover effects	• Activity from adjacent organs (gastrointestinal tract, lungs) or blood pool, masks, or distorts the actual myocardial signal.	• Might be challenging to identify. • Artificially elevated counts or apparent lower counts in myocardium. • Discordance between static and dynamic (motion and breathing-corrected) images.	• Adjust regions of interest on both static and dynamic images to exclude if possible, the extracardiac activity. • Interpret accordingly in cases where complete exclusion is not feasible (e.g. lung uptake adjacent to lateral wall)

perfusion defects (*Figure 21*). Of note, studies can have areas of both hibernating and scarred myocardium. When stress images are also obtained, FDG uptake can be seen in areas of reversible perfusion defects, a phenomenon called ischaemic memory (*Figure 22*). Since ^{15}O-water relies on quantitative, rather than qualitative, assessment, it cannot be used for viability imaging, which relies exclusively on the qualitative comparison of perfusion and FDG-imaging. Studies are underway to determine whether measures of MBF can be used to differentiate scar vs. hibernation, but this is largely pre-clinical.[82]

Viability imaging—artefacts and non-diagnostic studies

Artefacts due to soft tissue attenuation, patient motion and mis-registration can occur, emphasizing the need for adequate attenuation correction and quality control. Patient preparation for viability PET can be problematic in patients with Type 2 diabetes, who have underlying insulin resistance.[9,47] Lastly, the threshold of glucose uptake and number of segments that predict functional improvement is not well defined, as the literature is heterogeneous with mixed results. Decisions to pursue further therapy based on the results of viability testing require integration of other imaging modalities and the clinical context.

Viability imaging—hybrid PET and cardiac magnetic resonance imaging

PET and cardiac magnetic resonance imaging (CMR) are the two most advanced modalities for assessing hibernation. Rather than measuring metabolic activity, as in PET, contrast-enhanced CMR can assess for viability by measuring the degree of fibrosis and extracellular expansion where gadolinium accumulates to a greater extent than normal

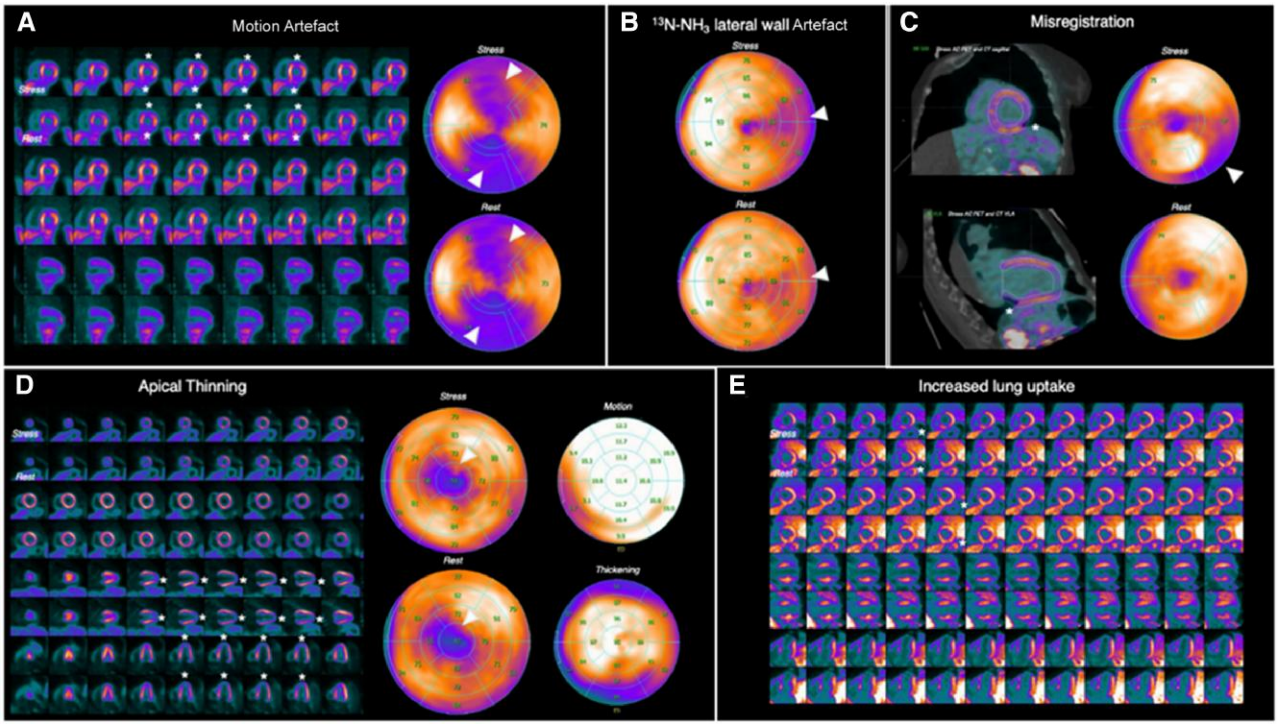

Figure 17 Demonstrative examples of the most common artefacts encountered at PET MPI. (*A*) Typical appearance of a motion artefact (butterfly appearance) evident at both stress and rest images of a restless patient with claustrophobia undergoing PET MPI. (*B*) Typical fixed lateral wall defect in a patient undergoing rest/stress ^{13}N-NH$_3$ PET MPI. Note that the defect is more evident at stress due to higher tracer dose applied. (*C*) Mis-registration of the stress PET images with the CT transmission images resulting in a reversible perfusion defect at the inferolateral basal wall. (*D*) Typical apical thinning defect at a patient undergoing PET MPI with normal wall motion and thickening. (*E*) Increased lung uptake at a patient undergoing rest/stress ^{13}N-NH$_3$ PET MPI directly after cigarette smoking. Note the more prominent extracardiac uptake during rest. *Asterisks depict the artefact at the slices, and arrow heads depict the corresponding artefact appearance at the polar plots.*

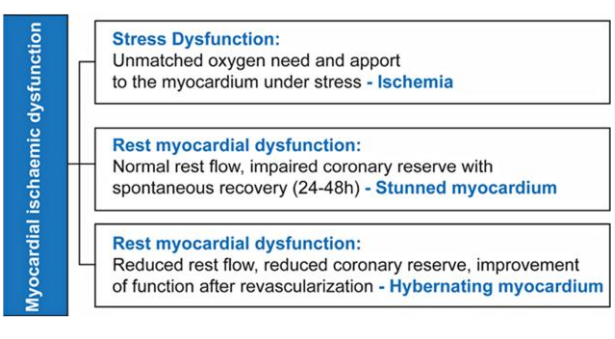

Figure 18 The spectrum of myocardial ischaemic dysfunction.

myocardium.[72] On CMR, myocardial segments for which there is >50% late gadolinium enhancement is considered scar and unlikely to recovery. Since PET and CMR rely on different techniques to assess viability, hybrid PET/CMR may provide a more accurate assessment of viability and aid in resolving discrepancies when traditional PET/CT and CMR are discordant.[83,84] However, further research is warranted to better understand the additive value of combining these two modalities.

Clinical Pearl #5	PET is more sensitive than SPECT for the detection of hibernating myocardium and is therefore the preferred modality when available.

CT for PET including incidental findings

Attenuation correction is required for interpretation of cardiac PET.[85] A CT scan is obtained either pre- and/or post the radiotracer emission scan with a field-of-view that includes the chest to avoid truncation artefacts. Patients must remain still to avoid mis-registration artefacts (*Figure 23*). To reduce radiation dose, CT performed for attenuation correction typically uses lower tube current and larger slice thickness than dedicated cardiac imaging, such as is used for calcium scores or coronary CT angiograms. The CT is performed without intravenous contrast, ECG-gating, or breath-holds. Consequently, this CT is not optimized for diagnostic chest imaging.

Despite the lower resolution, clinically actionable findings, both cardiac and non-cardiac, can be present and should be reported.[86] Common cardiac findings include coronary or valve calcification, which

Table 5 Common radiation dose to patients by different PET stress protocols and tracers

Study protocol	Radiotracer	Typically administrated activity (mCi/MBq)	Estimated radiation dose (mSv)
3D PET			
Rest + stress perfusion	^{82}Rb	20 + 20/*740* + *740*	2
Rest + stress perfusion	^{13}N-NH$_3$	10 + 10/370 + 370	2
Rest + stress perfusion	^{15}O-water	10 + 10/370 + 370	0.8
Rest perfusion + viability	^{82}Rb/^{18}F-FDG	20 + 5/740 + 185	2 + 3.5
Rest perfusion + viability	^{13}N-NH$_3$/^{18}F-FDG	10 + 5/370 + 185	2 + 3.5
2D PET			
Rest + stress perfusion	^{82}Rb	50 + 50/*1480* + *1480*	4
Rest + stress perfusion	^{13}N-NH$_3$	20 + 20/740 + 740	4
Rest + stress perfusion	^{15}O-water	30 + 30/1110 + 1110	2.4
Rest + stress perfusion	^{18}F-flurpiridaz	2.5–3.0 + 9.0–9.5/93–111 + 333–352[a]	7[a]
		2.5–3.0 + 6.0–6.5/93–333 + 222–241[b]	6.3[b]
Rest perfusion + viability	^{82}Rb/^{18}F-FDG	50 + 20/1480 + 375	4 + 7
Rest perfusion + viability	^{13}N-NH$_3$/^{18}F-FDG	20 + 10/375	4 + 7

Radiation dose does not include contribution from CT, which may vary based on type of scanner and whether concurrent calcium scoring is performed.[23,76–78]
[a]Flurpiridaz reported rest/stress doses for rest/exercise stress.
[b]Flurpiridaz reported rest/stress doses for rest/pharmacological stress.

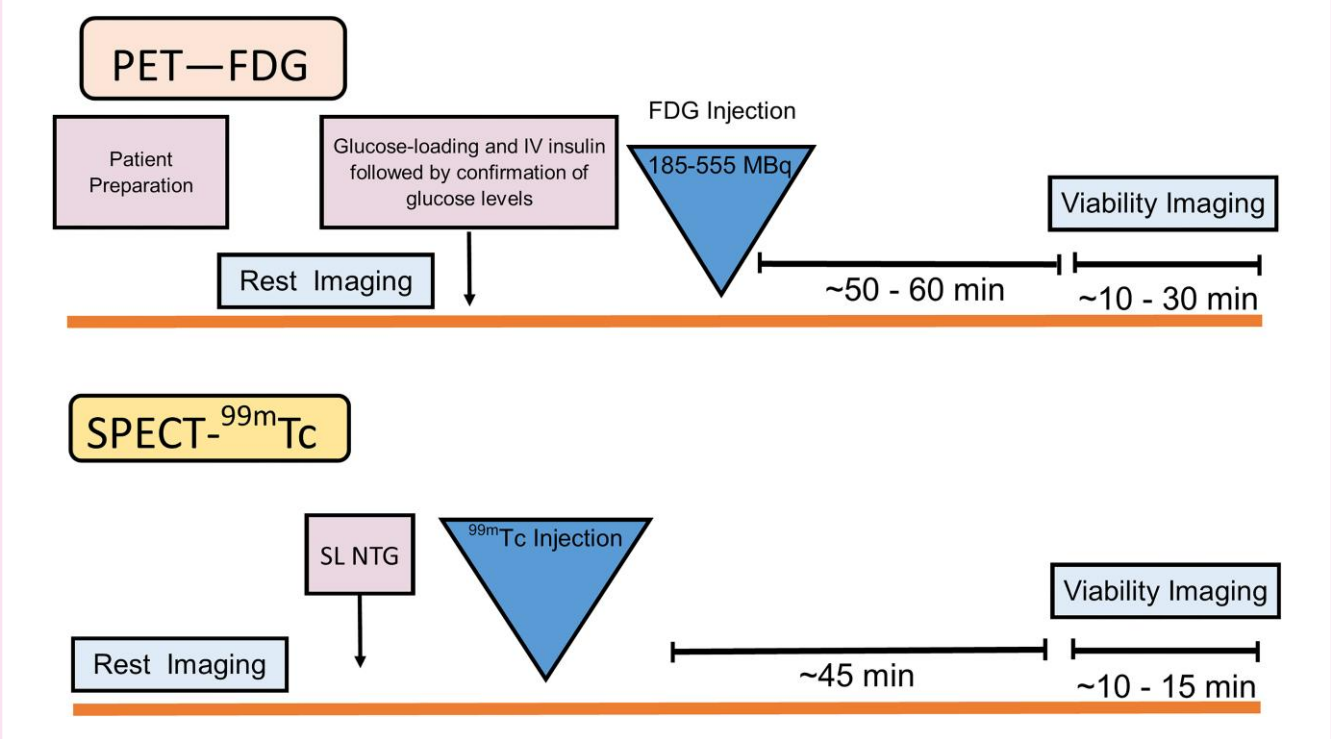

Figure 19 Examples of viability imaging protocols for PET with ^{18}F-FDG and SPECT with ^{99}m-technetium (^{99m}Tc). For FDG-PET (top), patients consume a low-fat meal the evening prior. Rest imaging is performed with traditional perfusion tracers. If there are fixed perfusion defects, the patient can proceed with viability imaging. Patients undergo glucose loading followed by injection of IV insulin to target goal serum glucose. FDG is then injected and viability imaging performed. Hibernating myocardium will have uptake of FDG. For SPECT (bottom), no dietary prep is necessary. After rest imaging demonstrates fixed perfusion defects, patients can undergo viability imaging. Nitroglycerine is administered prior to the second injection of technetium to augment MBF and tracer uptake. SL NTG, sublingual nitroglycerine.

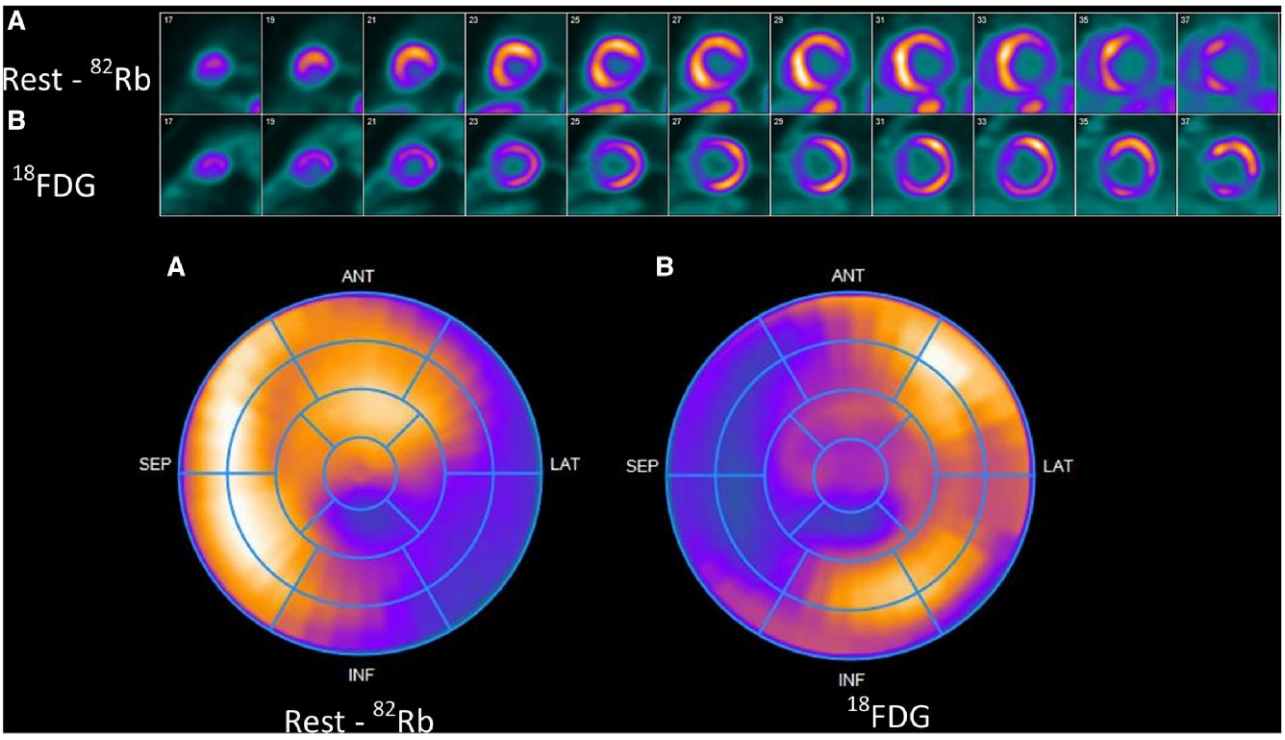

Figure 20 (*A*) Large fixed perfusion defect in the inferior and inferolateral segments on resting ^{82}Rb-chloride imaging. (*B*) Viability imaging shows FDG uptake in the inferior and inferolateral wall demonstrating hibernating myocardium.

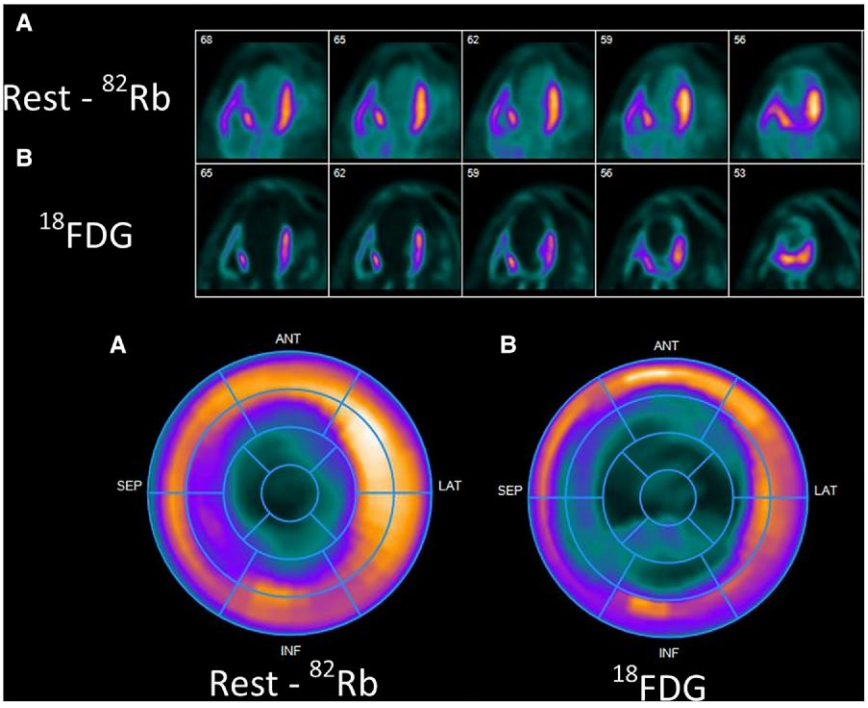

Figure 21 (*A*) Large fixed perfusion defect in a left anterior descending distribution on resting ^{82}Rb-chloride imaging. (*B*) Viability imaging shows no FDG uptake in these segments, demonstrating scar.

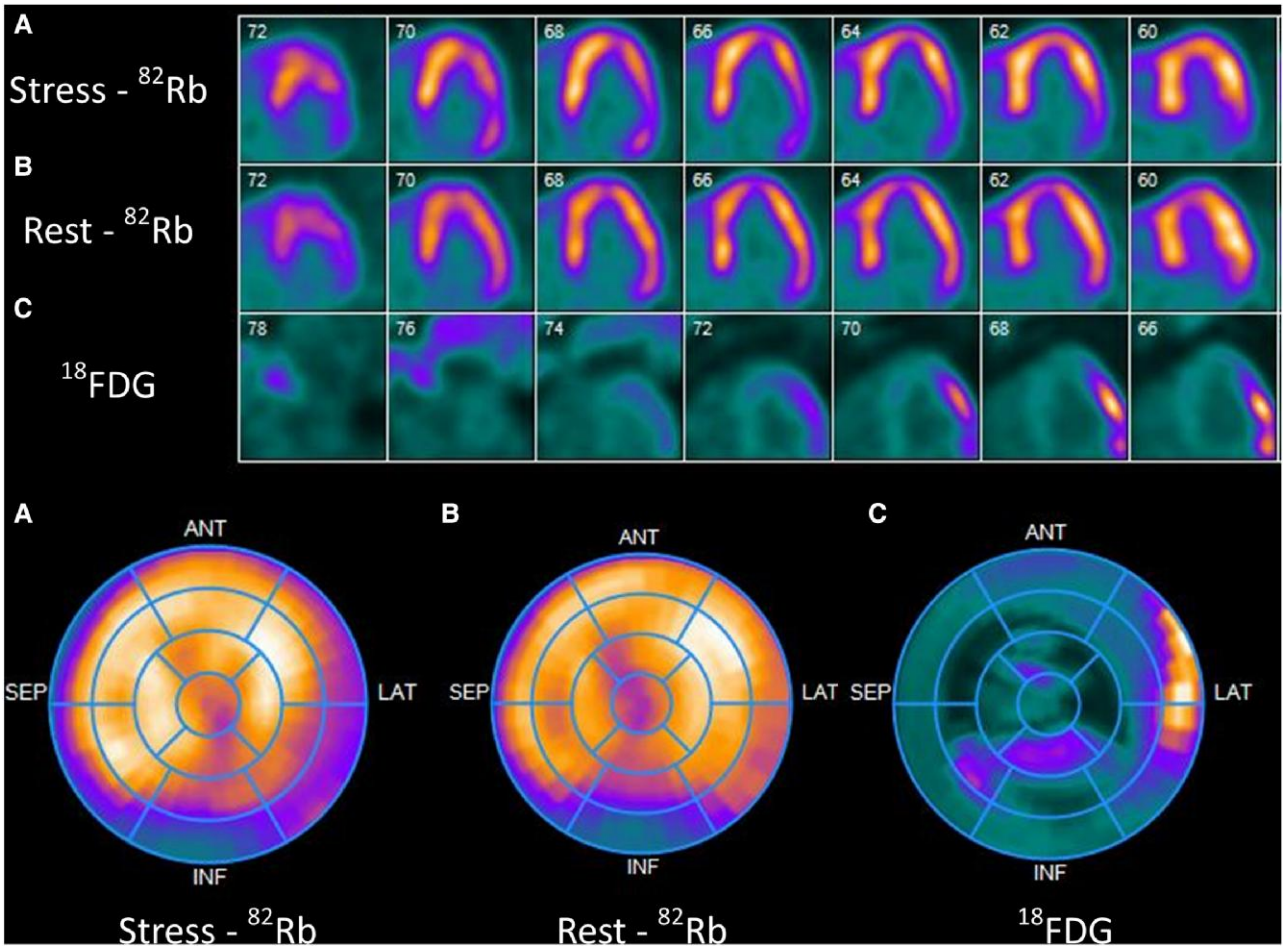

Figure 22 Stress/rest/viability imaging with ^{82}Rb. Stress (*A*) and rest (*B*) imaging shows a small, fixed defect in the inferior segments along with ischaemia in the lateral wall. (*C*) FDG images show scar in the inferior segments. FDG uptake in the lateral wall, corresponding to the ischaemic territory, is an example of ischaemic memory.

can be reported as either binary (present or absent) or according to qualitative categories (mild, moderate, and severe), and pericardial effusions (*Figure 24*). CT in cardiac PET includes the thoracic aorta and may identify patients with abnormal dilations (*Figure 25*). Hypoattenuation of the liver (<40 Hounsfield units) on non-contrast CT may signify non-alcoholic fatty liver disease which can provide additional prognostic information and change medical therapy.[87] Lung or breast findings are also common and can include masses, infiltrates, or pleural effusions (*Figure 24*). Many risk factors for cardiovascular disease also increase the risk of cancer, emphasizing the need for a thorough assessment of the CT data. Prior dedicated chest or cardiac CT can be reviewed to assess for interval change.

A dedicated coronary artery calcium score can be performed in patients without known CAD. Coronary calcium scoring requires prospective, ECG-gating with inspiratory breath-holds and therefore cannot be used for attenuation correction. Adding a coronary artery calcium score may improve specificity, as patients with low coronary artery calcium scores are less likely to have flow-limiting CAD. Coronary artery calcium scoring can provide additional prognostic value and should be integrated with the patient's age, sex, and traditional risk factors. The prognostic value of calcium scoring should not be applied to those with prior revascularization.[88]

Calcium scoring can also be used to guide medical management with the initiation of lipid-lowering therapies, such as statins, or antiplatelet medications.[89,90] Statin therapy slows atherosclerosis, but can convert non-calcified plaque to calcified plaque and therefore worsen calcium scores.[91] While calcium scoring continues to have prognostic value in patients on statins, the relationship is weaker compared with non-statin users.[92] Patient education is critical to ensure patients understand how their therapy may affect calcium scoring on serial MPI studies.

Clinical Pearl #6	Incidental CT findings can have significant impact on patient management, particularly the presence of coronary calcium. This may prompt changes in medical management of coronary artery disease, even in the absence of ischaemia.

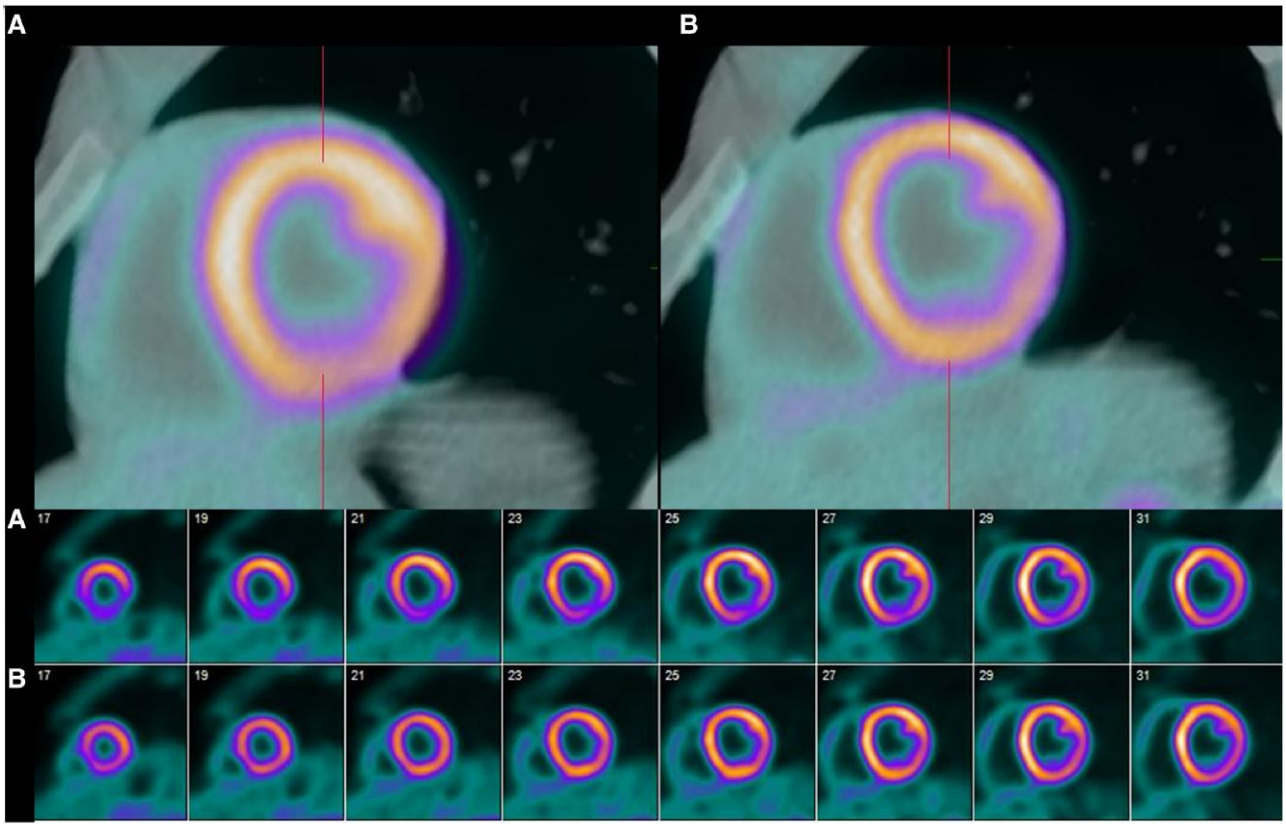

Figure 23 CT transmission-emission misalignment. Misalignment of CT transmission and ^{13}N-NH_3 emission scan inferiorly and inferolateral causes an apparent perfusion defect (*A*) that disappears with proper alignment (*B*).

Artificial intelligence and nuclear imaging

Artificial intelligence (AI) is being increasingly introduced into many aspects of cardiovascular imaging, including nuclear myocardial perfusion. The primary areas of ongoing advancement are image reconstruction, image interpretation, and prognostication.[93] Like iterative reconstruction, AI may be used in post-image processing to enhance signal to noise ratio and improve image resolution.[94] Retrospective studies have also shown promising AI models for direct image interpretation and prediction of major adverse cardiovascular events.[95,96] Prospective research is needed to best determine the generalizability and cost-effectiveness of various nuclear MPI AI models. A more detailed position paper on AI applications in nuclear imaging has been previously published by the EACVI.[97]

Generating a clinically meaningful report

A clinically meaningful report includes an assessment of image quality, interpretation of perfusion and gated images, quantification of MBF, evaluation of extracardiac findings, and finally, a clinical impression with risk-stratification (*Figure 26*).

Image quality should be reported, giving an impression of the readers' diagnostic confidence and artefacts that may limit the interpretation of the exam.

Perfusion imaging should be reported in standard approach with comment on the coronary distribution, defect size, and defect severity. Markers of high-risk, including transient ischaemic dilatation or a drop in left ventricular ejection fraction, should be noted. Chamber size and function from the gated images should be included. MBF is a key strength of PET MPI and can improve the sensitivity of the exam. MBF should be reported when data are available and of high quality.

Associated symptoms or ECG-changes during the exam may be clinically meaningful. A comment on coronary calcification by CT can also improve the diagnostic and prognostic value of the exam.

Finally, after combining the MPI, MBF, and non-MPI results, the reader should provide a personalized and actionable report for clinicians to integrate into their practice.

Figure 24 Incidental findings on CT performed for attenuation correction. (*A*) Coronary artery calcification (dotted line) and bilateral pleural effusions (solid line). (*B*) Breast mass (dotted line) and severe mitral annular calcification (solid line).

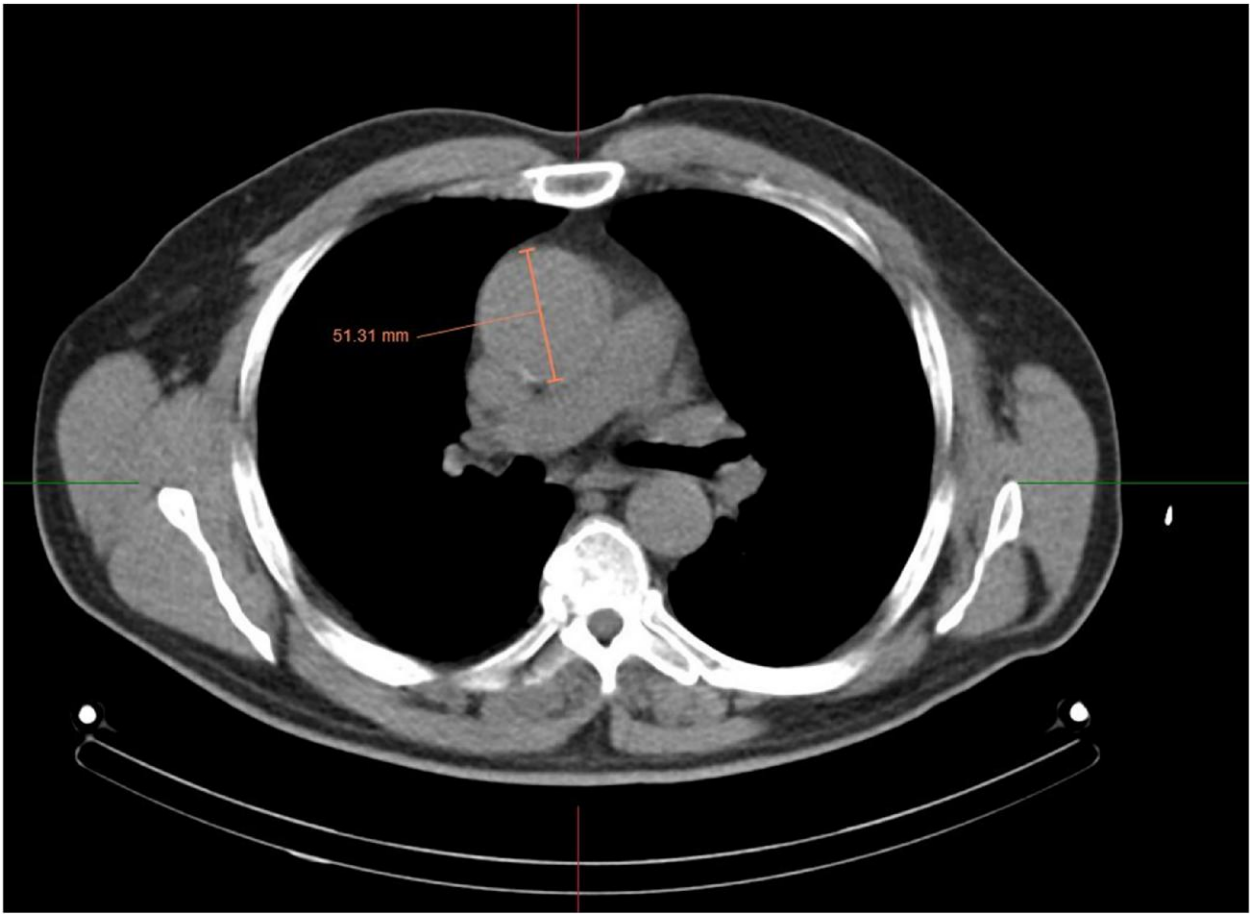

Figure 25 Incidentally found, aneurysmal dilation of the ascending aorta.

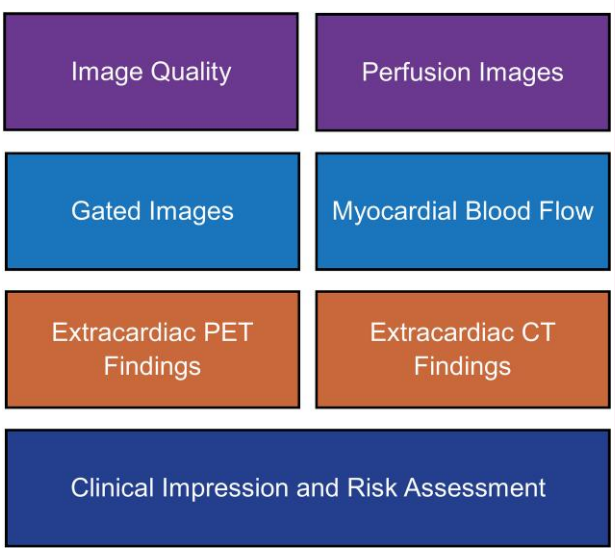

Figure 26 Pillars of a comprehensive PET-MPI report.

Conclusion

PET MPI is an advanced nuclear molecular imaging tool for the diagnosis and risk-stratification of CAD, as well as the assessment of scar and hibernation. This document provides a comprehensive overview of the technical aspects of PET MPI, with a focus on patient preparation, tracer characteristics, image acquisition and interpretation, and common pitfalls and artefacts that are encountered in daily practice.

Supplementary data

Supplementary data are available at *European Heart Journal—Imaging Methods and Practice* online.

Acknowledgements

This document was reviewed by members of the 2024–26 EACVI Scientific Documents Committee: Philippe Bertrand, Erwan Donal, Marc Dweck, Niall Keenan, Valtteri Uusitalo.

Conflict of interest: A.A.G. reports research grant support from GE Healthcare, the Iten-Kohaut Foundation, and Promedica Stiftung, has

given talks for GE Healthcare and has performed consultancy for Artrya Ltd. F.H. has received consultant and speaker fees from Bracco Imaging, Cisbio International, and GE healthcare, and he is a shareholder in Naogen Pharma. A.S. has received fees for lectures or consultancy from Abbot, Astra Zeneca, BMS, Janssen, Novo Nordisk, and Pfizer. W.A.J. is on the board of directors of the executive council of the American Society of Nuclear Cardiology. The remainder authors have no relevant disclosures.

Funding

There is no funding for this study.

Data availability

No new data were generated or analysed in support of this research.

Lead author biography

Dr Bryan Abadie is an Associate Staff at the Cleveland Clinic Heart, Vascular, and Thoracic Institute. His clinical and research interest is multimodality imaging, including nuclear cardiology, echocardiography, cardiac magnetic resonance imaging, and cardiac computed tomography angiography.

References

1. Vrints C, Andreotti F, Koskinas KC, Rossello X, Adamo M, Ainslie J *et al.* 2024 ESC guidelines for the management of chronic coronary syndromes. *Eur Heart J* 2024;**45**:3415–537.
2. Gulati M, Levy PD, Mukherjee D, Amsterdam E, Bhatt DL, Birtcher KK *et al.* 2021 AHA/ACC/ASE/CHEST/SAEM/SCCT/SCMR guideline for the evaluation and diagnosis of chest pain: a report of the American College of Cardiology/American Heart Association joint committee on clinical practice guidelines. *Circulation* 2021;**144**:e368–454.
3. Multimodality Writing Group for Chronic Coronary Disease; Winchester DE, Maron DJ, Blankstein R, Chang IC, Kirtane AJ *et al.* ACC/AHA/ASE/ASNC/ASPC/HFSA/HRS/SCAI/SCCT/SCMR/STS 2023 multimodality appropriate use criteria for the detection and risk assessment of chronic coronary disease. *J Am Coll Cardiol* 2023;**81**:2445–67.
4. Abadie B, Liga R, Buechel R, Giannopoulos AA, Pizzi MN, Roque A *et al.* Patient centric performance and interpretation of SPECT and SPECT/CT myocardial perfusion imaging: a clinical consensus statement of the European Association of Cardiovascular Imaging of the ESC. *Eur Heart J Imaging Methods Pract* 2025;**3**:345.
5. Renaud JM, Yip K, Guimond J, Trottier M, Pibarot P, Turcotte E *et al.* Characterization of 3-dimensional PET systems for accurate quantification of myocardial blood flow. *J Nucl Med* 2017;**58**:103–9.
6. van Dijk JD, Jager PL, van Osch JAC, Khodaverdi M, van Dalen JA. Comparison of maximal Rubidium-82 activities for myocardial blood flow quantification between digital and conventional PET systems. *J Nucl Cardiol* 2019;**26**:1286–91.
7. Henzlova MJ, Duvall WL, Einstein AJ, Travin MI, Verberne HJ. ASNC imaging guidelines for SPECT nuclear cardiology procedures: stress, protocols, and tracers. *J Nucl Cardiol* 2016;**23**:606–39.
8. Gibbons RJ, Balady GJ, Beasley JW, Bricker JT, Duvernoy WFC, Froelicher VF *et al.* ACC/AHA guidelines for exercise testing: executive summary. A report of the American College of Cardiology/American Heart Association task force on practice guidelines (committee on exercise testing). *Circulation* 1997;**96**:345–54.
9. Dorbala S, Ananthasubramaniam K, Armstrong IS, Chareonthaitawee P, DePuey EG, Einstein AJ *et al.* Single Photon Emission Computed Tomography (SPECT) myocardial perfusion imaging guidelines: instrumentation, acquisition, processing, and interpretation. *J Nucl Cardiol* 2018;**25**:1784–846.
10. Verberne HJ, Acampa W, Anagnostopoulos C, Ballinger J, Bengel F, De Bondt P *et al.* EANM procedural guidelines for radionuclide myocardial perfusion imaging with SPECT and SPECT/CT: 2015 revision. *Eur J Nucl Med Mol Imaging* 2015;**42**:1929–40.
11. Hoffmeister C, Preuss R, Weise R, Burchert W, Lindner O. The effect of beta blocker withdrawal on adenosine myocardial perfusion imaging. *J Nucl Cardiol* 2014;**21**:1223–9.
12. Yoon AJ, Melduni RM, Duncan S-A, Ostfeld RJ, Travin MI. The effect of beta-blockers on the diagnostic accuracy of vasodilator pharmacologic SPECT myocardial perfusion imaging. *J Nucl Cardiol* 2009;**16**:358–67.
13. Reyes E, Stirrup J, Roughton M, D'Souza S, Underwood SR, Anagnostopoulos C. Attenuation of adenosine-induced myocardial perfusion heterogeneity by atenolol and other cardioselective β-adrenoceptor blockers: a crossover myocardial perfusion imaging study. *J Nucl Med* 2010;**51**:1036–43.
14. Koepfli P, Wyss CA, Namdar M, Klainguti M, von Schulthess GK, Lüscher TF *et al.* Beta-adrenergic blockade and myocardial perfusion in coronary artery disease: differential effects in stenotic versus remote myocardial segments. *J Nucl Med* 2004;**45**:1626–31.
15. Hajjiri MM, Leavitt MB, Zheng H, Spooner AE, Fischman AJ, Gewirtz H. Comparison of positron emission tomography measurement of adenosine-stimulated absolute myocardial blood flow versus relative myocardial tracer content for physiological assessment of coronary artery stenosis severity and location. *JACC Cardiovasc Imaging* 2009;**2**:751–8.
16. Murthy VL, Bateman TM, Beanlands RS, Berman DS, Borges-Neto S, Chareonthaitawee P *et al.* Clinical quantification of myocardial blood flow using PET: joint position paper of the SNMMI cardiovascular council and the ASNC. *J Nucl Med* 2018;**59**:273–93.
17. Sciagrà R, Lubberink M, Hyafil F, Saraste A, Slart RHJA, Agostini D *et al.* EANM procedural guidelines for PET/CT quantitative myocardial perfusion imaging. *Eur J Nucl Med Mol Imaging* 2021;**48**:1040–69.
18. Tsj O, Rjj K, Jh C, M W, Fm VZ. Myocardial blood flow and myocardial flow reserve values in (13)N-ammonia myocardial perfusion PET/CT using a time-efficient protocol in patients without coronary artery disease. *Eur J Hybrid Imaging* 2018;**2**:11.
19. Markousis-Mavrogenis G, Juárez-Orozco LE, Alexanderson E. Residual activity correction in quantitative myocardial perfusion (13)N-ammonia pet imaging: a study in post-mi patients. *Hellenic J Cardiol* 2017;**58**:245–9.
20. FDA. *FDA Approves Imaging Drug for Evaluation of Myocardial Ischemia and Infarction*. FDA; 2024. https://www.fda.gov/drugs/news-events-human-drugs/fda-approves-imaging-drug-evaluation-myocardial-ischemia-and-infarction.
21. Krajewski S, Steczek L, Gotowicz K, Karczmarczyk U, Towpik J, Witkowska-Patena E *et al.* Preclinical evaluation of [(18)F]SYN1 and [(18)F]SYN2, novel radiotracers for PET myocardial perfusion imaging. *EJNMMI Res* 2024;**14**:63.
22. Conti M, Eriksson L. Physics of pure and non-pure positron emitters for PET: a review and a discussion. *EJNMMI Phys* 2016;**3**:8.
23. Maddahi J, Agostini D, Bateman TM, Bax JJ, Beanlands RSB, Berman DS *et al.* Flurpiridaz F-18 PET myocardial perfusion imaging in patients with suspected coronary artery disease. *J Am Coll Cardiol* 2023;**82**:1598–610.
24. Maddahi J, Lazewatsky J, Udelson JE, Berman DS, Beanlands RSB, Heller GV *et al.* Phase-III clinical trial of fluorine-18 flurpiridaz positron emission tomography for evaluation of coronary artery disease. *J Am Coll Cardiol* 2020;**76**:391–401.
25. Maddahi J, Packard RR. Cardiac PET perfusion tracers: current status and future directions. *Semin Nucl Med* 2014;**44**:333–43.
26. Prior JO, Allenbach G, Valenta I, Kosinski M, Burger C, Verdun FR *et al.* Quantification of myocardial blood flow with 82Rb positron emission tomography: clinical validation with 15O-water. *Eur J Nucl Med Mol Imaging* 2012;**39**:1037–47.
27. Abadie BQ, Chan N, Sharalaya Z, Bhat P, Harb S, Jacob M *et al.* Negative predictive value and prognostic associations of Rb-82 PET/CT with myocardial blood flow in CAV. *JACC Heart Fail* 2023;**11**:555–65.
28. Dietz M, Kamani CH, Allenbach G, Rubimbura V, Fournier S, Dunet V *et al.* Comparison of the prognostic value of impaired stress myocardial blood flow, myocardial flow reserve, and myocardial flow capacity on low-dose Rubidium-82 SiPM PET/CT. *J Nucl Cardiol* 2023;**30**:1385–95.
29. Kajander S, Joutsiniemi E, Saraste M, Pietilä M, Ukkonen H, Saraste A *et al.* Cardiac positron emission tomography/computed tomography imaging accurately detects anatomically and functionally significant coronary artery disease. *Circulation* 2010;**122**:603–13.
30. Flotats A, Knuuti J, Gutberlet M, Marcassa C, Bengel FM, Kaufmann PA *et al.* Hybrid cardiac imaging: SPECT/CT and PET/CT. A joint position statement by the European Association of Nuclear Medicine (EANM), the European Society of Cardiac Radiology (ESCR) and the European Council of Nuclear Cardiology (ECNC). *Eur J Nucl Med Mol Imaging* 2011;**38**:201–12.
31. Dorbala S, Di Carli MF, Delbeke D, Abbara S, DePuey EG, Dilsizian V *et al.* SNMMI/ASNC/SCCT guideline for cardiac SPECT/CT and PET/CT 1.0. *J Nucl Med* 2013;**54**:1485–507.
32. Shepp LA, Vardi Y. Maximum likelihood reconstruction for emission tomography. *IEEE Trans Med Imaging* 1982;**1**:113–22.
33. Hudson HM, Larkin RS. Accelerated image reconstruction using ordered subsets of projection data. *IEEE Trans Med Imaging* 1994;**13**:601–9.
34. Slomka PJ, Moody JB, Miller RJH, Renaud JM, Ficaro EP, Garcia EV. Quantitative clinical nuclear cardiology, part 2: evolving/emerging applications. *J Nucl Med* 2021;**62**:168–76.
35. Garcia EV, Slomka P, Moody JB, Germano G, Ficaro EP. Quantitative clinical nuclear cardiology, part 1: established applications. *J Nucl Med* 2019;**60**:1507–16.

36. Tilkemeier PL, Bourque J, Doukky R, Sanghani R, Weinberg RL. ASNC imaging guidelines for nuclear cardiology procedures: standardized reporting of nuclear cardiology procedures. *J Nucl Cardiol* 2017;**24**:2064–128.
37. Chareonthaitawee P, Bateman TM, Beanlands RS, Berman DS, Calnon DA, Di Carli MF *et al.* Atlas for reporting PET myocardial perfusion imaging and myocardial blood flow in clinical practice: an information statement from the American Society of Nuclear Cardiology. *J Nucl Cardiol* 2023;**30**:2850–906.
38. Trägårdh E, Hesse B, Knuuti J, Flotats A, Kaufmann PA, Kitsiou A *et al.* Reporting nuclear cardiology: a joint position paper by the European Association of Nuclear Medicine (EANM) and the European Association of Cardiovascular Imaging (EACVI). *Eur Heart J Cardiovasc Imaging* 2015;**16**:272–9.
39. Cerqueira MD, Weissman NJ, Dilsizian V, Jacobs AK, Kaul S, Laskey WK *et al.* Standardized myocardial segmentation and nomenclature for tomographic imaging of the heart. A statement for healthcare professionals from the Cardiac Imaging Committee of the Council on Clinical Cardiology of the American Heart Association. *Circulation* 2002;**105**:539–42.
40. Hickey KT, Sciacca RR, Bokhari S, Rodriguez O, Chou R-L, Faber TL *et al.* Assessment of cardiac wall motion and ejection fraction with gated PET using N-13 ammonia. *Clin Nucl Med* 2004;**29**:243–8.
41. Juarez-Orozco LE, Monroy-Gonzalez A, Prakken NHJ, Noordzij W, Knuuti J, deKemp RA *et al.* Phase analysis of gated PET in the evaluation of mechanical ventricular synchrony: a narrative overview. *J Nucl Cardiol* 2019;**26**:1904–13.
42. Schaefer WM, Lipke CSA, Standke D, Kühl HP, Nowak B, Kaiser HJ *et al.* Quantification of left ventricular volumes and ejection fraction from gated ^{99m}Tc-MIBI SPECT: MRI validation and comparison of the emory cardiac tool box with QGS and 4D-MSPECT. *J Nucl Med* 2005;**46**:1256–63.
43. Bateman TM, Heller GV, Beanlands R, Calnon DA, Case J, deKemp R *et al.* Practical guide for interpreting and reporting cardiac PET measurements of myocardial blood flow: an information statement from the American Society of Nuclear Cardiology, and the Society of Nuclear Medicine and Molecular Imaging. *J Nucl Med* 2021;**62**:1599–615.
44. Schindler TH, Fearon WF, Pelletier-Galarneau M, Ambrosio G, Sechtem U, Ruddy TD *et al.* Myocardial perfusion PET for the detection and reporting of coronary microvascular dysfunction: a JACC: cardiovascular imaging expert panel statement. *JACC Cardiovasc Imaging* 2023;**16**:536–48.
45. Pelletier-Galarneau M, Martineau P, El Fakhri G. Quantification of PET myocardial blood flow. *Curr Cardiol Rep* 2019;**21**:11.
46. Danad I, Uusitalo V, Kero T, Saraste A, Raijmakers PG, Lammertsma AA *et al.* Quantitative assessment of myocardial perfusion in the detection of significant coronary artery disease: cutoff values and diagnostic accuracy of quantitative [^{15}O]H_2O PET imaging. *J Am Coll Cardiol* 2014;**64**:1464–75.
47. Singh V, Dorbala S. Normal variants and pitfalls in cardiac PET/CT. *Semin Nucl Med* 2021;**51**:441–57.
48. Lim P, Agarwal V, Patel KK. How to assess nonresponsiveness to vasodilator stress. *J Nucl Cardiol* 2024;**36**:101850.
49. Saad JM, Ahmed AI, Han Y, El Nihum LI, Alahdab F, Nabi F *et al.* Splenic switch-off in regadenoson (82)Rb-PET myocardial perfusion imaging: assessment of clinical utility. *J Nucl Cardiol* 2023;**30**:1484–96.
50. Alnabelsi T, Thakkar A, Ahmed AI, Han Y, Al-Mallah MH. PET/CT myocardial perfusion imaging acquisition and processing: ten tips and tricks to help you succeed. *Curr Cardiol Rep* 2021;**23**:39.
51. Martinez-Möller A, Souvatzoglou M, Navab N, Schwaiger M, Nekolla SG. Artifacts from misaligned CT in cardiac perfusion PET/CT studies: frequency, effects, and potential solutions. *J Nucl Med* 2007;**48**:188–93.
52. Rajaram M, Tahari AK, Lee AH, Lodge MA, Tsui B, Nekolla S *et al.* Cardiac PET/CT misregistration causes significant changes in estimated myocardial blood flow. *J Nucl Med* 2013;**54**:50–4.
53. Votaw JR, Packard RRS. Technical aspects of acquiring and measuring myocardial blood flow: method, technique, and QA. *J Nucl Cardiol* 2018;**25**:665–70.
54. Lassen ML, Rasmussen T, Byrne C, Holmvang L, Kjaer A, Hasbak P. Myocardial creep and cardiorespiratory motion correction improves diagnostic accuracy of Rubidium-82 cardiac positron emission tomography. *J Nucl Cardiol* 2023;**30**:2289–300.
55. Kuronuma K, Wei C-C, Singh A, Lemley M, Hayes SW, Otaki Y *et al.* Automated motion correction for myocardial blood flow measurements and diagnostic performance of (82)Rb PET myocardial perfusion imaging. *J Nucl Med* 2024;**65**:139–46.
56. Kuronuma K, Miller RJH, Wei CC, Singh A, Lemley MH, Van Kriekinge SD *et al.* Downward myocardial creep during stress PET imaging is inversely associated with mortality. *Eur J Nucl Med Mol Imaging* 2024;**51**:1622–31.
57. Tout D, Tonge CM, Muthu S, Arumugam P. Assessment of a protocol for routine simultaneous myocardial blood flow measurement and standard myocardial perfusion imaging with rubidium-82 on a high count rate positron emission tomography system. *Nucl Med Commun* 2012;**33**:1202–11.
58. Klein R, Adler A, Beanlands RS, Dekemp RA. Precision-controlled elution of a 82Sr/82Rb generator for cardiac perfusion imaging with positron emission tomography. *Phys Med Biol* 2007;**52**:659–73.
59. Alzahrani AH, Arasaratnam P, Massalha S, Alenazy A, Lee A, Clarkin O *et al.* Effect of proton pump inhibitors on Rubidium-82 gastric uptake using positron emission tomography myocardial perfusion imaging. *J Nucl Cardiol* 2020;**27**:1443–51.
60. Rasmussen T, Kjær A, Hasbak P. Stomach interference in (82)Rb-PET myocardial perfusion imaging. *J Nucl Cardiol* 2019;**26**:1934–42.
61. Steffen DA, Giannopoulos AA, Grossmann M, Messerli M, Schwyzer M, Gräni C *et al.* "Apical thinning": relations between myocardial wall thickness and apical left ventricular tracer uptake as assessed with positron emission tomography myocardial perfusion imaging. *J Nucl Cardiol* 2020;**27**:452–60.
62. Tomiyama T, Ishihara K, Suda M, Kanaya K, Sakurai M, Takahashi N *et al.* Impact of time-of-flight on qualitative and quantitative analyses of myocardial perfusion PET studies using (13)N-ammonia. *J Nucl Cardiol* 2015;**22**:998–1007.
63. Koenders SS, van Dijk JD, Jager PL, Ottervanger JP, Slump CH, van Dalen JA. Impact of regadenoson-induced myocardial creep on dynamic Rubidium-82 PET myocardial blood flow quantification. *J Nucl Cardiol* 2019;**26**:719–28.
64. Beanlands RS, Muzik O, Hutchins GD, Wolfe ER Jr, Schwaiger M. Heterogeneity of regional nitrogen 13-labeled ammonia tracer distribution in the normal human heart: comparison with rubidium 82 and copper 62-labeled PTSM. *J Nucl Cardiol* 1994;**1**:225–35.
65. de Jong RM, Blanksma PK, Willemsen AT, Anthonio RL, Meeder JG, Pruim J *et al.* Posterolateral defect of the normal human heart investigated with nitrogen-13-ammonia and dynamic PET. *J Nucl Med* 1995;**36**:581–5.
66. Klingensmith WC III, Noonan C, Goldberg JH, Buchwald D, Kimball JT, Manson SM. Decreased perfusion in the lateral wall of the left ventricle in PET/CT studies with 13N-ammonia: evaluation in healthy adults. *J Nucl Med Technol* 2009;**37**:215–9.
67. Dilsizian V, Bacharach SL, Beanlands RS, Bergmann SR, Delbeke D, Dorbala S *et al.* ASNC imaging guidelines/SNMMI procedure standard for positron emission tomography (PET) nuclear cardiology procedures. *J Nucl Cardiol* 2016;**23**:1187–226.
68. Juneau D, Ruddy TD, Beanlands RSB, deKemp RA. False-positive (13)N-ammonia positron emission tomography perfusion scan caused by misalignment of adjacent lung activity during attenuation correction. *J Nucl Cardiol* 2018;**25**:1056–8.
69. Hoff CM, Sørensen J, Kero T, Bouchelouche K, Harms HJ, Frøkiær J *et al.* Quantitative and qualitative comparison of Rubidium-82 and Oxygen-15 water cardiac PET. *J Nucl Cardiol* 2024;**32**:101796.
70. Bol A, Melin JA, Vanoverschelde JL, Baudhuin T, Vogelaers D, De Pauw M *et al.* Direct comparison of [^{13}N]ammonia and [^{15}O]water estimates of perfusion with quantification of regional myocardial blood flow by microspheres. *Circulation* 1993;**87**:512–25.
71. Ryan M, Morgan H, Chiribiri A, Nagel E, Cleland J, Perera D. Myocardial viability testing: all STICHed up, or about to be REVIVED? *Eur Heart J* 2022;**43**:118–26.
72. Garcia MJ, Kwong RY, Scherrer-Crosbie M, Taub CC, Blankstein R, Lima J *et al.* State of the art: imaging for myocardial viability: a scientific statement from the American Heart Association. *Circ Cardiovasc Imaging* 2020;**13**:e000053.
73. Almeida AG, Carpenter J-P, Cameli M, Donal E, Dweck MR, Flachskampf FA *et al.* Multimodality imaging of myocardial viability: an expert consensus document from the European Association of Cardiovascular Imaging (EACVI). *Eur Heart J Cardiovasc Imaging* 2021;**22**:e97–125.
74. Panza JA, Chrzanowski L, Bonow RO. Myocardial viability assessment before surgical revascularization in ischemic cardiomyopathy. *J Am Coll Cardiol* 2021;**78**:1068–77.
75. Neumann F-J, Sousa-Uva M, Ahlsson A, Alfonso F, Banning AP, Benedetto U *et al.* 2018 ESC/EACTS guidelines on myocardial revascularization. *EuroIntervention* 2019;**14**:1435–534.
76. Desiderio MC, Lundbye JB, Baker WL, Farrell MB, Jerome SD, Heller GV. Current status of patient radiation exposure of cardiac positron emission tomography and single-photon emission computed tomographic myocardial perfusion imaging. *Circ Cardiovasc Imaging* 2018;**11**:e007565.
77. Gimelli A, Achenbach S, Buechel RR, Edvardsen T, Francone M, Gaemperli O *et al.* Strategies for radiation dose reduction in nuclear cardiology and cardiac computed tomography imaging: a report from the European Association of Cardiovascular Imaging (EACVI), the Cardiovascular Committee of European Association of Nuclear Medicine (EANM), and the European Society of Cardiovascular Radiology (ESCR). *Eur Heart J* 2018;**39**:286–96.
78. Case JA, deKemp RA, Slomka PJ, Smith MF, Heller GV, Cerqueira MD. Status of cardiovascular PET radiation exposure and strategies for reduction: an information statement from the cardiovascular PET task force. *J Nucl Cardiol* 2017;**24**:1427–39.
79. Shah NR, Dorbala S, Dilsizian V. *Positron Emission Tomography Assessment of Myocardial Viability*. ASNC. Published online ahead of print. https://www.asnc.org/wp-content/uploads/2024/05/Positron-Emission-Tomography-Assessment-of-Myocardial-ViabilityaE%E2%80%B9.pdf.
80. Mhlanga J, Derenoncourt P, Haq A, Bhandiwad A, Laforest R, Siegel BA *et al.* ^{18}F-FDG PET in myocardial viability assessment: a practical and time-efficient protocol. *J Nucl Med* 2022;**63**:602–8.
81. Castellucci P, Deandreis D, Krizsan A, Mirzaei S, Prior J, Sattler B *et al.* Myocardial viability. In: European Nuclear Medicine Guide. EANM/UEMS/EBNM; 2020. https://eanm.org/publications/useful-resources/nuclear-medicine-guide/.

82. Grönman M, Tarkia M, Stark C, Vähäsilta T, Kiviniemi T, Lubberink M *et al.* Assessment of myocardial viability with [(15)O]water PET: a validation study in experimental myocardial infarction. *J Nucl Cardiol* 2021;**28**:1271–80.
83. Kazimierczyk R, Kaminski KA, Nekolla SG. Cardiac PET/MRI: recent developments and future aspects. *Semin Nucl Med* 2024;**54**:733–46.
84. Vitadello T, Kunze KP, Nekolla SG, Langwieser N, Bradaric C, Weis F *et al.* Hybrid PET/MR imaging for the prediction of left ventricular recovery after percutaneous revascularisation of coronary chronic total occlusions. *Eur J Nucl Med Mol Imaging* 2020;**47**:3074–83.
85. Alessio AM, Kohlmyer S, Branch K, Chen G, Caldwell J, Kinahan P. Cine CT for attenuation correction in cardiac PET/CT. *J Nucl Med* 2007;**48**:794–801.
86. Kay FU, Canan A, Abbara S. Common incidental findings on cardiac CT: a systematic review. *Curr Cardiovasc Imaging Rep* 2019;**12**, Article 21.
87. Kodama Y, Ng CS, Wu TT, Ayers GD, Curley SA, Abdalla EK *et al.* Comparison of CT methods for determining the fat content of the liver. *AJR Am J Roentgenol* 2007;**188**:1307–12.
88. Golub IS, Termeie OG, Kristo S, Schroeder LP, Lakshmanan S, Shafter AM *et al.* Major global coronary artery calcium guidelines. *JACC Cardiovasc Imaging* 2023;**16**:98–117.
89. Mouden M, Timmer JR, Reiffers S, Oostdijk AHJ, Knollema S, Ottervanger JP *et al.* Coronary artery calcium scoring to exclude flow-limiting coronary artery disease in symptomatic stable patients at low or intermediate risk. *Radiology* 2013;**269**:77–83.
90. Engbers EM, Timmer JR, Ottervanger JP, Mouden M, Knollema S, Jager PL. Prognostic value of coronary artery calcium scoring in addition to single-photon emission computed tomographic myocardial perfusion imaging in symptomatic patients. *Circ Cardiovasc Imaging* 2016;**9**:e003966.
91. Lee S-E, Chang H-J, Sung JM, Park H-B, Heo R, Rizvi A *et al.* Effects of statins on coronary atherosclerotic plaques: the PARADIGM study. *JACC Cardiovasc Imaging* 2018;**11**:1475–84.
92. Osei AD, Mirbolouk M, Berman D, Budoff MJ, Miedema MD, Rozanski A *et al.* Prognostic value of coronary artery calcium score, area, and density among individuals on statin therapy vs. non-users: the coronary artery calcium consortium. *Atherosclerosis* 2021;**316**:79–83.
93. Fortuni F, Ciliberti G, De Chiara B, Conte E, Franchin L, Musella F *et al.* Advancements and applications of artificial intelligence in cardiovascular imaging: a comprehensive review. *Eur Heart J Imaging Methods Pract* 2024;**2**:qyae136.
94. Golub IS, Thummala A, Morad T, Dhaliwal J, Elisarraras F, Karlsberg RP *et al.* Artificial intelligence in nuclear cardiac imaging: novel advances, emerging techniques, and recent clinical trials. *J Clin Med* 2025;**14**:2095.
95. Apostolopoulos ID, Apostolopoulos DI, Spyridonidis TI, Papathanasiou ND, Panayiotakis GS. Multi-input deep learning approach for cardiovascular disease diagnosis using myocardial perfusion imaging and clinical data. *Phys Med* 2021;**84**:168–77.
96. Betancur J, Otaki Y, Motwani M, Fish MB, Lemley M, Dey D *et al.* Prognostic value of combined clinical and myocardial perfusion imaging data using machine learning. *JACC Cardiovasc Imaging* 2018;**11**:1000–9.
97. Slart RHJA, Williams MC, Juarez-Orozco LE, Rischpler C, Dweck MR, Glaudemans AWJM *et al.* Position paper of the EACVI and EANM on artificial intelligence applications in multimodality cardiovascular imaging using SPECT/CT, PET/CT, and cardiac CT. *Eur J Nucl Med Mol Imaging* 2021;**48**:1399–413.